

## Original Article

# HMGB1/STAT3/p65 axis drives microglial activation and autophagy exert a crucial role in chronic Stress-Induced major depressive disorder

Ke Xu<sup>a,b</sup>, Mingyang Wang<sup>c</sup>, Haiyang Wang<sup>b,d</sup>, Shuang Zhao<sup>e</sup>, Dianji Tu<sup>f</sup>, Xue Gong<sup>b</sup>, Wenxia Li<sup>b</sup>, Xiaolei Liu<sup>g</sup>, Lianmei Zhong<sup>g,\*</sup>, Jianjun Chen<sup>h,\*</sup>, Peng Xie<sup>a,b,\*</sup>

<sup>a</sup> Department of Neurology, The First Affiliated Hospital of Chongqing Medical University, Chongqing 400016, China

<sup>b</sup> National Health Commission Key Laboratory of Diagnosis and Treatment on Brain Functional Diseases, The First Affiliated Hospital of Chongqing Medical University, Chongqing 400016, China

<sup>c</sup> Kunming Institute of Zoology, Chinese Academy of Sciences, Kunming 650223, China

<sup>d</sup> Key Laboratory of Psychosomatics, Stomatological Hospital of Chongqing Medical University, Chongqing 401147, China

<sup>e</sup> Department of Pathophysiology, Chongqing Medical University, Chongqing 400016, China

<sup>f</sup> Department of Clinical Laboratory, Xinqiao Hospital, Third Military Medical University, Chongqing 400037, China

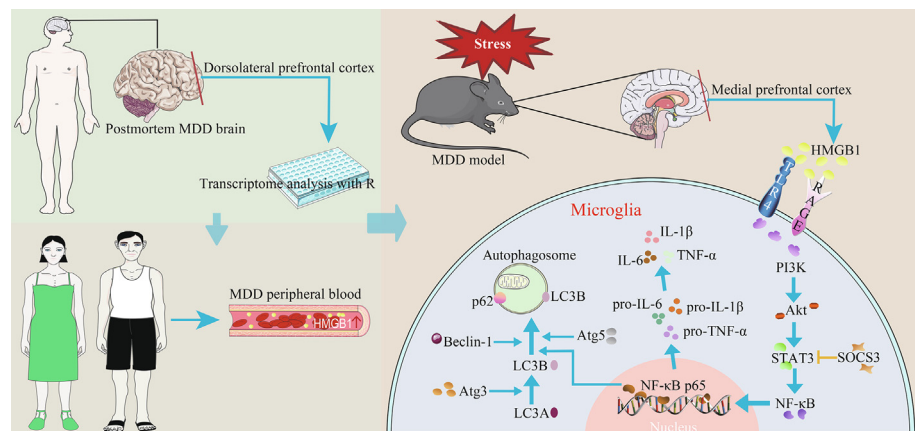
<sup>g</sup> Department of Neurology, The First Affiliated Hospital of Kunming Medical University, Kunming 650032, China

<sup>h</sup> Institute of Life Sciences, Chongqing Medical University, Chongqing 400016, China

## HIGHLIGHTS

- HMGB1/STAT3/p65 axis mediated microglial activation and autophagy in mPFC correlated with MDD were first identified, and HMGB1 was found to be a potential biomarker for MDD.
- Increased HMGB1 expression was mainly observed in microglia from the medial prefrontal cortex of MDD model mice.
- Specific knockdown of HMGB1 rescues chronic stress-induced depressive-related phenotypes, microglial activation, and autophagy in mice.
- The effects induced by chronic stress were mimicked by exogenous administration of recombinant HMGB1 or specific overexpression of HMGB1, while blocked by STAT3 specific inhibitor or p65 knockdown.
- Inhibition of HMGB1/STAT3/p65 axis prevented LPS-induced microglial activation and autophagy *in vitro*, which was reversed by recombinant HMGB1 protein overexpression.
- Microglial HMGB1/STAT3/p65 axis within the mPFC is a novel therapeutic target in the treatment of MDD associated with stress.

## GRAPHICAL ABSTRACT



\* Corresponding authors at: Department of Neurology, The First Affiliated Hospital of Kunming Medical University, 295 Xichang Road, Kunming 650032, China (L. Zhong) Institute of Life Sciences, Chongqing Medical University, No.1 Yixueyuan Road, Yuzhong District, Chongqing 400016, China (J. Chen) National Health Commission Key Laboratory of Diagnosis and Treatment on Brain Functional Diseases, The First Affiliated Hospital of Chongqing Medical University, No.1 Yixueyuan Road, Yuzhong District, Chongqing 400016, China (P. Xie).

E-mail addresses: [13888967787@163.com](mailto:13888967787@163.com) (L. Zhong), [chenjianjun@cqmu.edu.cn](mailto:chenjianjun@cqmu.edu.cn) (J. Chen), [xiepeng@cqmu.edu.cn](mailto:xiepeng@cqmu.edu.cn) (P. Xie).

<https://doi.org/10.1016/j.jare.2023.06.003>

2090-1232/2024 The Authors. Published by Elsevier B.V. on behalf of Cairo University.

This is an open access article under the CC BY-NC-ND license (<http://creativecommons.org/licenses/by-nc-nd/4.0/>).

## ARTICLE INFO

## Article history:

Received 8 August 2022

Revised 4 May 2023

Accepted 8 June 2023

Available online 13 June 2023

## Keywords:

Major depressive disorder

Medial prefrontal cortex

Microglial

HMGB1/STAT3/p65 axis

Neuroinflammation

Autophagy

## ABSTRACT

**Introduction:** Neuroinflammation and autophagy are implicated in stress-related major depressive disorder (MDD), but the underlying molecular mechanisms remain largely unknown.

**Objectives:** Here, we identified that MDD regulated by HMGB1/STAT3/p65 axis mediated microglial activation and autophagy for the first time. Further investigations were performed to uncover the effects of this axis on MDD *in vivo* and *in vitro*.

**Methods:** Bioinformatics analyses were used to re-analysis the transcriptome data from the dorsolateral prefrontal cortex (dlPFC) of post-mortem male MDD patients. The expression level of HMGB1 and its correlation with depression symptoms were explored in MDD clinical patients and chronic social defeat stress (CSDS)-induced depression model mice. Specific adeno-associated virus and recombinant (r) HMGB1 injection into the medial PFC (mPFC) of mice, and pharmacological inhibitors with rHMGB1 in two microglial cell lines exposed to lipopolysaccharide were used to analyze the effects of HMGB1/STAT3/p65 axis on MDD.

**Results:** The differential expression of genes from MDD patients implicated in microglial activation and autophagy regulated by HMGB1/STAT3/p65 axis. Serum HMGB1 level was elevated in MDD patients and positively correlated with symptom severity. CSDS not only induced depression-like states in mice, but also enhanced microglial reactivity, autophagy as well as activation of the HMGB1/STAT3/p65 axis in mPFC. The expression level of HMGB1 was mainly increased in the microglial cells of CSDS-susceptible mice, which also correlated with depressive-like behaviors. Specific HMGB1 knockdown produced a depression-resilient phenotype and suppressed the associated microglial activation and autophagy effects of CSDS-induced. The effects induced by CSDS were mimicked by exogenous administration of rHMGB1 or specific overexpression of HMGB1, while blocked by STAT3 inhibitor or p65 knockdown. *In vitro*, inhibition of HMGB1/STAT3/p65 axis prevented lipopolysaccharide-induced microglial activation and autophagy, while rHMGB1 reversed these changes.

**Conclusion:** Our study established the role of microglial HMGB1/STAT3/p65 axis in mPFC in mediating microglial activation and autophagy in MDD.

© 2024 The Authors. Published by Elsevier B.V. on behalf of Cairo University. This is an open access article under the CC BY-NC-ND license (<http://creativecommons.org/licenses/by-nc-nd/4.0/>).

## Introduction

Major depressive disorder (MDD) is a debilitating mental illness with an estimated global life-time prevalence of 21% [1]. Numerous risk alleles for MDD have been identified, but onset is closely associated with environmental factors, such as stressful life events. The dorsolateral prefrontal cortex (dlPFC) of MDD patients is reduced in thickness, neuronal and glial cell densities, and individual cell size [2]. Moreover, MDD model mice established by chronic stress exhibit both functional and morphological abnormalities in the medial PFC (mPFC) [3], the equivalent of the primate dlPFC [4].

Sustained stress and the subsequent release of pro-inflammatory cytokines lead to chronic neuroinflammation and dysregulated autophagy, which in turn are associated with MDD [5,6]. Indeed, the neuroinflammatory factor lipopolysaccharide (LPS) can also induce depressive-like behavior, underscoring the importance of neuroinflammation and possible autophagic impairment to MDD etiology [7]. Meanwhile, autophagy has been recognized as a marker for the development of MDD [8]. Brain-resident macrophages (microglia) are essential mediators of neuroinflammation in response to stress, and thus microglial activation is considered a major pathogenic process contributing to MDD [9]. And microglial activation-mediated neuroinflammation has been found in MDD patients [10]. High mobility group box 1 (HMGB1) is a danger-associated molecular pattern molecule released in response to physical and psychological stressors. It contains 215 amino acid (aa) residues that form an acidic C-terminal tail (186–215 aa), and two homologous DNA-binding domains (A/B boxes, 1–79 aa, 89–162 aa). Extracellular stimulation induces pro-inflammatory signals in the B-box, whereas antagonistic effects are induced by the A-box [11]. Moreover, HMGB1 may function as a pro-inflammatory mediator by transducing extracellular signals through interactions with multiple receptors. While residues 150–183 interact with the receptor of advanced glycation end-products (RAGE) to activate inflammation signaling, residues 89–108 bind to toll-like receptor 4 (TLR4) and boost pro-inflammatory signaling [12]. Despite the interaction between neuroinflammation and autophagy is sophisti-

cated and controversial, neuroinflammation is implicated in autophagic dysfunction, and HMGB1 also acts as a regulator of autophagy in microglia [13]. Growing evidence indicates that chronic unpredictable mild stress (CUMS) upregulates HMGB1 in the hippocampus [14], and that it acts as a late-phase mediator of LPS-induced depression [15]. However, it remains unclear how elevated brain HMGB1 influences mPFC function and depressive-like behavior.

In this study, based on a re-analysis of MDD patient gene expression profiles available from the public database, we speculated that stress-induced activation of the HMGB1/signal transducer and activator of transcription 3 (STAT3)/nuclear factor-kappa B (NF-κB) p65 axis in the mPFC contributed to MDD pathogenesis by driving local microglial activation and autophagy. We also collected human blood samples to determine whether serum HMGB1 concentration was correlated with the clinical severity of MDD. Moreover, we used an animal model of chronic social defeat stress (CSDS)-induced depression-like states *in vivo* and the LPS-stimulated microglial cells *in vitro*. CSDS is a well-validated stress model of MDD that differentiates between susceptible and resilient mouse populations [16], in accord with the heterogeneous clinical outcomes observed among human populations under stress [17]. Using viral transfection, pharmacological inhibitors, and the recombinant protein to investigate if the microglial HMGB1/STAT3/p65 axis mediates stress-induced depressive-like behaviors as well as microglial activation and autophagy *in vivo* and *in vitro*. Our findings uncovered a previously unrecognized mechanism by which microglial HMGB1 activation in mPFC drives disease progression in MDD, suggesting potential utility as a therapeutic target for MDD treatment.

## Materials and methods

## Ethics statement

All experiments were performed according to the ethical policies in compliance with the ARRIVE guidelines and approved by the Ethics Committee of Chongqing Medical University

(No.2017013). Written consent was obtained from each MDD patient and healthy donor prior to blood sampling.

#### Postmortem human brain study

Whole-transcriptome total RNA expression profiles used in this study were obtained from Gene Expression Omnibus (GEO) dataset GSE101521, which included dlPFC expression results from male and female sudden-death medication-free individuals with no psychiatric conditions (controls), MDD without suicide (MDD), and MDD with suicide (MDDS) [18]. To rule out the potential effects of estrogen and the menstrual period, we excluded the female samples. After excluding the female sample data, the profile dataset included 42 specimens, 23 from controls, six from MDD patients, and 13 from MDDS patients (Supplementary Table S1). The limma package in R was applied to identify differentially expressed genes (DEGs), which were then mapped by Ingenuity Pathway Analysis (IPA) software (Valencia, CA, US) for functional analysis. IPA was also used to generate gene networks predicting pathways [19] associated with MDD. See [Supplementary Information](#) for further details.

#### Human serum samples

The study cohort included 39 drug-naïve MDD (DN-MDD) patients, 38 MDD patients with relapse or current drug treatment (DT-MDD), and 40 healthy control subjects (HCs). The inclusion and exclusion criteria were shown in [Supplementary Information](#). The clinical and demographic characteristics of recruited subjects are summarized in [Supplementary Table S2](#).

#### Animals

Adult male C57BL/6J mice (6–8 weeks of age) were purchased from ENSIWEIER Laboratory Animal Co. Ltd. (Chongqing, China). In the Animal Resource Centre of Chongqing Medical University, mice were housed single-caged with free access to food and water under standard conditions (12 h/12 h, light/dark cycle,  $23 \pm 2$  °C).

#### Real-time polymerase chain reaction (RT-qPCR)

Gene expression levels were measured by RT-qPCR as described in our previous publication [20] using  $\beta$ -actin as the internal control. Primer sequences in detail are shown in [Supplementary Table S3](#). The recombinant (r)HMGB1 (R&D Systems, Minneapolis, US) was dissolved in phosphate-buffered saline.

The enzyme-linked immunosorbent assay (ELISA), CSDS protocol, behavioral tests, immunohistochemistry, cell culture, cell viability assay, immunofluorescence staining and morphometric analysis, western blotting, stereotaxic injection, hematoxylin-eosin (HE) staining, BrdU and terminal deoxynucleotidyl transferase dUTP nick end labeling (TUNEL) immunofluorescent staining, autophagy flux assessment, and statistical analysis were performed as described in detail in the [Supplementary Information](#).

## Results

#### Analysis of depression-associated DEGs from postmortem human brain

Comparison of expression data between MDD patients and controls from the GEO database identified 232 DEGs in MDD patients (171 upregulated and 61 downregulated; [Supplementary Table S4](#)), while comparison of expression data between MDDS

patients and controls revealed 21 DEGs in MDDS patients (20 upregulated and 1 downregulated; [Supplementary Table S5](#)). Of these DEGs, four upregulated genes were shared by MDD and MDDS patients versus controls ([Fig. 1a](#)), RP11-742 N3.1, RPE65, IL-1A, and Tmprss3. The heat maps of the top 50 DEGs between MDD and control groups, and all 21 DEGs between MDDS and control groups are displayed in [Fig. 1b](#) and [1c](#), respectively.

Among the top 10 biological processes for the 232 DEGs between MDD and control groups were 'response to LPS' and 'glial cell development' ([Fig. 1d](#)), while genes associated with 'cellular response to TNF' were enriched among DEGs between MDDS and control groups ([Fig. 1e](#)). Moreover, IPA analysis of the respective top 20 enriched canonical pathways among DEGs between MDD and control groups ([Fig. 1f](#)) and between MDDS and control groups ([Fig. 1g](#)) yielded six co-enrichment pathways ([Fig. 1h](#)). For these pathways, IPA indicated potential links among MDD, signaling pathways involving HMGB1, NF- $\kappa$ B, TLR, and STAT3, and pro-inflammatory cytokines including IL-1 $\alpha/\beta$  and TNF ([Fig. 1i](#)). And the association of MDD with microglial activation and autophagy may be mediated by regulation of the HMGB1/STAT3/RELA (NF- $\kappa$ B p65) axis and ensuing IL-1 $\beta$ , IL-6, and TNF in the dlPFC ([Fig. 1j](#)).

#### Human serum HMGB1 is positively correlated with MDD clinical severity

Considering that HMGB1 may play a major role in the pathogenesis of MDD, we investigated the association between serum HMGB1 and MDD symptoms. Compared to HCs, DN-MDD and DT-MDD patients both exhibited significantly elevated serum HMGB1 ( $P < 0.001$ ; [Fig. 2a](#)). Receiver operating characteristic (ROC) analyses indicated that serum HMGB1 level could distinguish HCs from both DN-MDD (area under the ROC curve (AUC) = 0.8269,  $P < 0.0001$ ; [Fig. 2b](#)) and DT-MDD (AUC = 0.8796,  $P < 0.0001$ ; [Fig. 2c](#)). Meanwhile, the results of ROC showed that serum HMGB1 level could distinguish HCs from MDD (AUC = 0.8529,  $P < 0.0001$ ; [Supplementary Fig. S1a](#)); while it could not distinguish DT-MDD from DN-MDD (AUC = 0.6181,  $P > 0.05$ ; [Supplementary Fig. S1b](#)). Considering that the ROC curve was a graphical plot used to show the diagnostic ability of binary classifiers, thus we further used Classification and Regression Tree (CART) analysis to assess whether HMGB1 could distinguish between DN-MDD, DT-MDD, and HCs. The results showed that HMGB1 could not effectively separate the three groups: predictive accuracies of 50.63%, 35.78%, and 41.30% for HCs, DN-MDD, and DT-MDD ([Supplementary Fig. S1c](#)). Moreover, multiple regression ([Supplementary Table S6](#)) and Pearson correlation ( $r = 0.5322$ ,  $P < 0.0001$ ; [Fig. 2d](#)) analyses revealed that there was a significant positive correlation between serum HMGB1 level and depression symptom severity, indicating that patients with higher HMGB1 have a severe degree of depression.

#### Increased HMGB1 expression in the mPFC of susceptible mice is associated with depression-related behaviors

To further examine the results proposed by the bioinformatics analysis, we first examined where is HMGB1 normally expressed in the brain region using immunohistochemistry and immunofluorescence assays. As shown in [Supplementary Figure S2](#), a and b, the HMGB1 expression was not specific to any brain region or cell type in the mPFC region of mouse brain. Meanwhile, with the help of The Human Protein Atlas, we found that HMGB1 shows low human brain cell type specificity, and, in the cerebral cortex, appears at the highest staining in glial cells ([Supplementary Fig. S2c](#)). We then established MDD model mice by exposure to CSDS, followed by a battery of behavioral tests and biochemical assays ([Fig. 3a](#)). Based

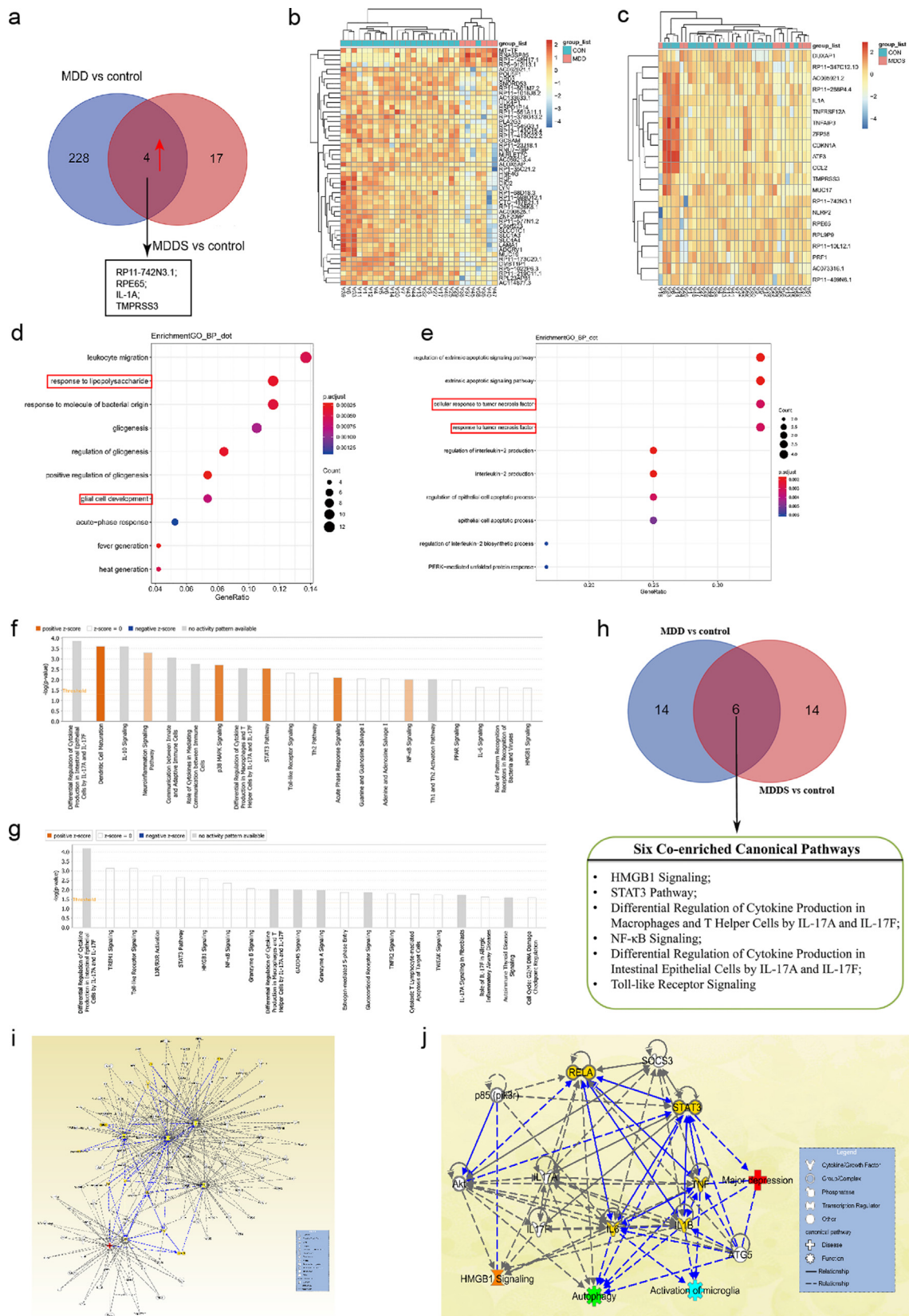


**Fig. 1.** Major depressive disorder (MDD) may be associated with HMGB1/STAT3/p65 axis-mediated microglial activation and autophagy in the dorsal lateral prefrontal cortex. (a) Venn diagram of differentially expressed genes (DEGs) between groups. Four upregulated DEGs were shared by MDD and MDD with suicide (MDDS) patients versus controls. (b, c) Heatmap of the top 50 DEGs between MDD patients and controls (b) and the 21 DEGs between MDDS patients and controls. (c). (d, e) Top 10 enriched gene ontology (GO) terms on “biological process” for DEGs between MDD and control groups (d) and between the MDDS and control groups (e). (f, g) Top 20 ingenuity pathway functional enrichment of DEGs between MDD and control groups (f) and between the MDDS and control groups (g). (h) Venn diagram of the top 20 enriched pathways for MDD vs. control groups and MDDS vs. control groups, and the 6 co-enriched (shared) pathways. (i) Potential relationships among MDD, HMGB1 signaling, Toll-like receptor signaling, NF-κB signaling, and STAT3 signaling. (j) Potential molecular networks linking MDD, autophagy, activation of microglia, IL-1β, IL-6, TNF, and the HMGB1/STAT3/RELA (NF-κB p65) axis.

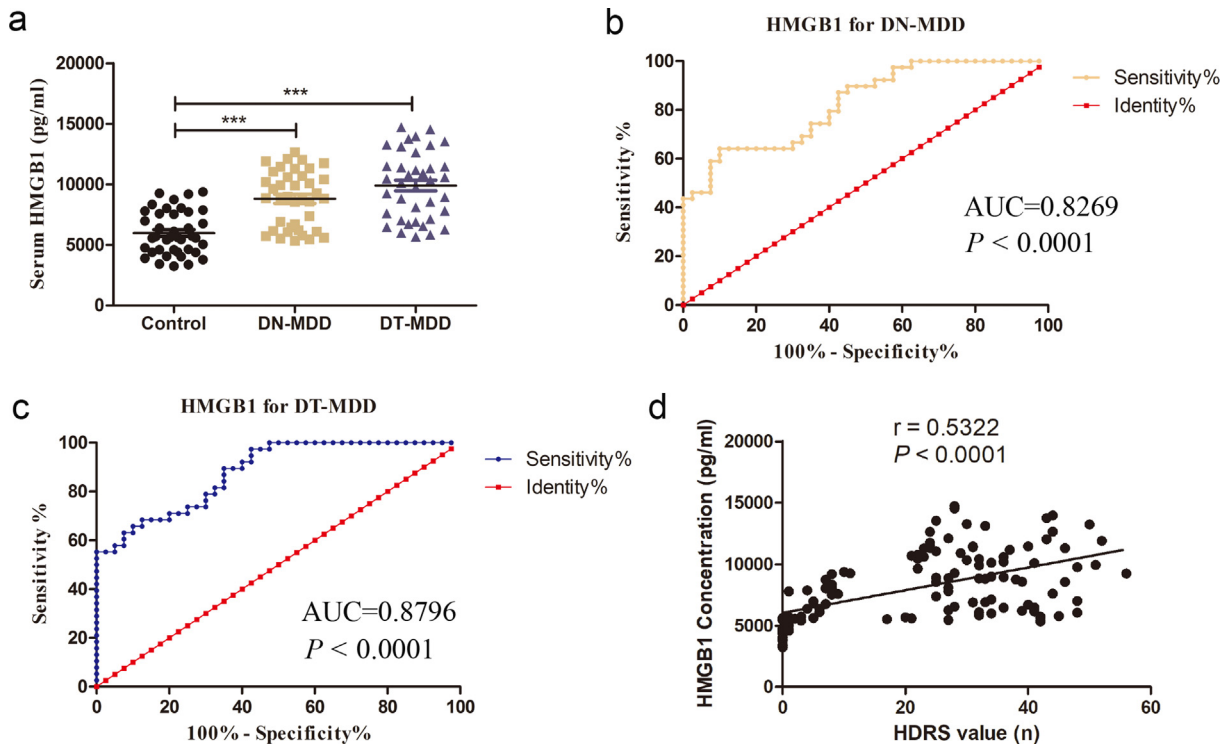


**Fig. 2.** Serum HMGB1 level predicts major depressive disorder (MDD) symptom severity. (a) Serum HMGB1 levels in healthy controls ( $n = 40$ ), drug-naive MDD patients (DN-MDD;  $n = 39$ ), and MDD patients with relapse or current drug treatment (DT-MDD;  $n = 38$ ). (b, c) ROC curves of HMGB1 for DN-MDD (b) and DT-MDD (c) diagnosis. (d) Pearson correlation between serum HMGB1 concentration and MDD symptom severity HDRS value. Detection limit of the ELISA: 10 pg/ml. Data are presented as mean  $\pm$  S.E. M. \*\*\* $P < 0.001$  vs. healthy controls. AUC, area under the ROC curve; ROC, receiver operating characteristic.

on social interaction (SI) ratios, stress-exposed mice were divided into susceptible and resilient subgroups.

Compared to unstressed-control mice, susceptible mice demonstrated significantly lower SI ratios and time in the interaction zone ( $P < 0.01$ ; Fig. 3b). Susceptible mice also displayed greater anhedonia in the sucrose preference test (SPT;  $P < 0.01$ ; Fig. 3c), and anxiety-like behaviors in the elevated plus maze test (decreased number of entries into the open arm and total time in the open arm;  $P < 0.05$ ; Fig. 3d) and in the open field test (OFT; decreased number of rearings and distance traveled in the center zone;  $P < 0.05$ ; Fig. 3e). Moreover, susceptible mice displayed higher immobility time in the tail suspension test (TST;  $P < 0.05$ ; Fig. 3f). However, there were no significant differences in SI (SI ratio, time in the interaction zone with no target, and time in the interaction zone with target), SPT (sucrose preference), elevated plus maze test (number of entries into the open arm, total time in the open arm), OFT (total distance, number of rearings, and distance traveled in the center zone), and TST (immobility time) between control and resilient groups (all  $P > 0.05$ ).

Both HMGB1 mRNA and protein levels in mPFC were significantly higher in susceptible mice (both  $P < 0.05$ ; Fig. 3g, h) but not in resilient mice compared to controls. Pearson correlation analysis (Fig. 3i–p) showed that HMGB1 mRNA levels were significantly negatively correlated with sucrose preference ( $r = -0.5976$ ,  $P = 0.0186$ ; Fig. 3j) and the number of rearings ( $r = -0.6207$ ,  $P = 0.0135$ ; Fig. 3m), but positively correlated with immobility time in the TST ( $r = 0.6421$ ,  $P = 0.0099$ ; Fig. 3p). These data demonstrate that HMGB1 expression increased the susceptibility to stress-induced depressive-like behaviors in mice.

#### CSDS promotes HMGB1/STAT3/p65 axis expression, microglial activation, and autophagy in the mPFC of susceptible mice

We have shown that enhanced expression of HMGB1 in mPFC is associated with depression-related behaviors in CSDS mice. Next, we thought to determine the critical cell type in which HMGB1 is acting to produce the effects. Thus, we examined the expression of HMGB1 in mPFC of stress-susceptible mice brain using immunofluorescence staining with specific cell makers. As shown in Fig. 4a, we found that in the stress-susceptible mouse brain, the increased expression of HMGB1 was mainly observed in microglia (Iba1 labeled), relative to astrocytes (GFAP labeled) and neurons (NeuN labeled), suggesting that HMGB1 in microglial of mPFC plays an important role in chronic stress-induced depression. Moreover, the expression levels of key downstream proteins of HMGB1 were measured by western blot, and we found that RAGE, TLR4, PI3K p85, p-Akt/Akt, p-STAT3/STAT3, and p-p65/p65 were significantly increased, whereas the expression level of suppressor of cytokine signaling 3 (SOCS3), a negative regulator of STAT3, was decreased in susceptible mice (all  $P < 0.05$ ; Fig. 4b, c). Chronic stress also increased the mRNA levels of IL-1 $\beta$  and IL-6 in the mPFC of susceptible mice (both  $P < 0.05$ ; Fig. 4d, e), though there was no significant difference in TNF- $\alpha$  expression between groups ( $P > 0.05$ ; Fig. 4f).

Immunofluorescence and Sholl analyses revealed that CSDS caused hyper-ramification of microglia in the mPFC of susceptible mice, characterized by significantly increased fluorescence intensity of activation marker Iba1, cell density, and branch interactions ( $P < 0.05$ ; Fig. 5a–d). CSDS also promoted the protein level of Iba1 in susceptible mice ( $P < 0.05$ ; Fig. 5e). Additionally, expression levels of the autophagy biomarkers Atg3, Atg5, Beclin-1, and

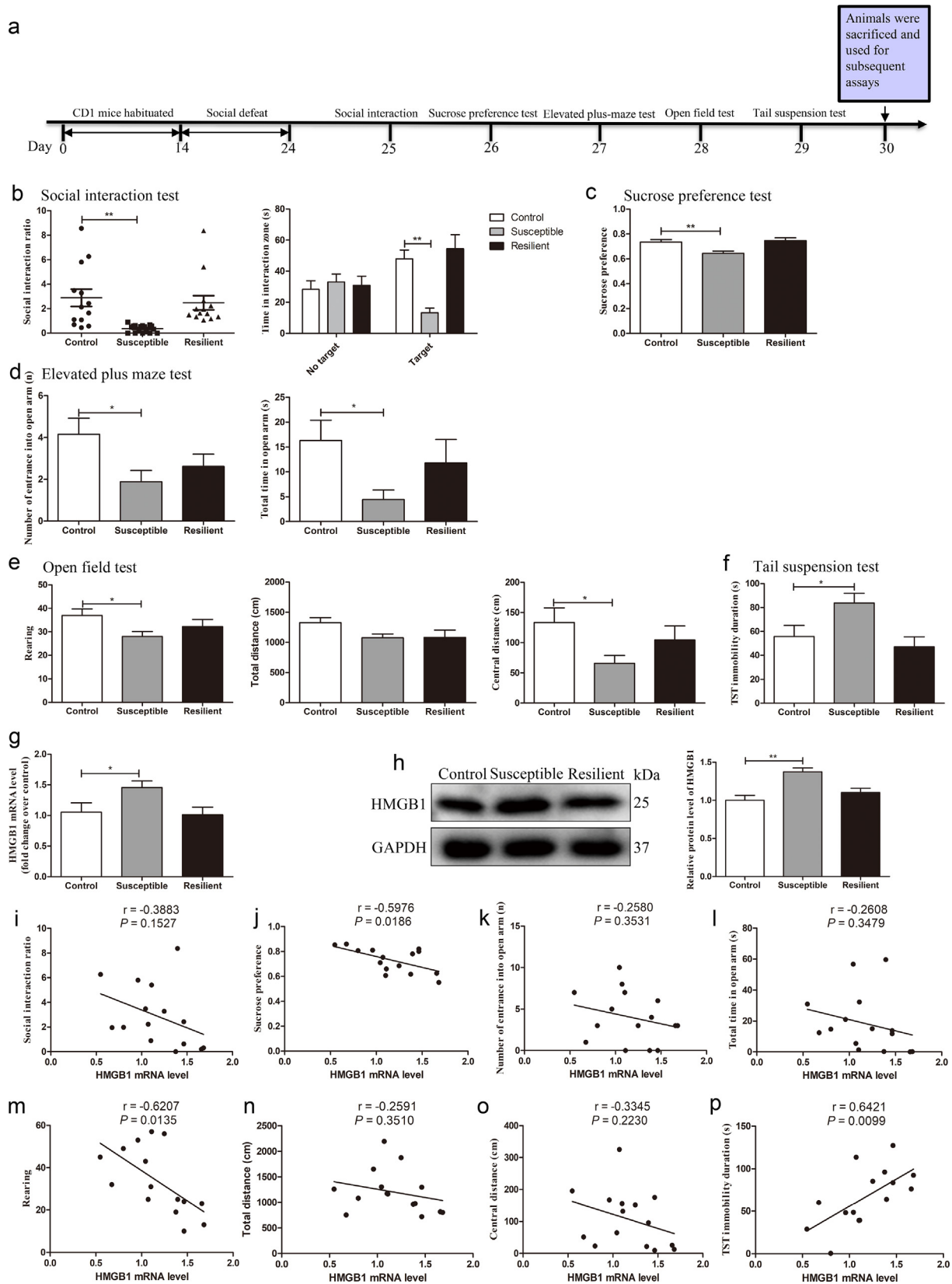


**Fig. 3.** Correlation analysis between depressive-like behaviors and HMGB1 level in the mPFC of chronic social defeat stress (CSDS) model mice. (a) Experimental timeline of CSDS. (b–f) Social interaction ratio and time in the interaction zone (b), sucrose preference (c), number of entries into the open arm and total time spent in the open arm of elevated plus maze test (d), number of rearings, total distance traveled, and distance traveled in the center zone during the 5-min open field test (e), and immobility time in the tail suspension test (TST; f) for control mice ( $n = 13$ ), CSDS-treated susceptible mice ( $n = 17$ ), and CSDS-treated resilient mice ( $n = 13$ ). (g) RT-qPCR analysis of HMGB1 mRNA expression in the mPFC ( $n = 5$  per group). (h) HMGB1 protein expression level in the mPFC ( $n = 4$  per group). (i–p) Pearson correlation analysis between HMGB1 mRNA level and depressive-like behaviors ( $n = 5$  per group), including social interaction ratio (i), sucrose preference (j), number of entries into the open arm (k), total time spent in the open arm (l), number of rearings (m), total distance traveled (n), distance traveled in the center zone (o), and immobility time in the TST (p). Data are presented as mean  $\pm$  SEM. \* $P < 0.05$ , \*\* $P < 0.01$  vs. control group.

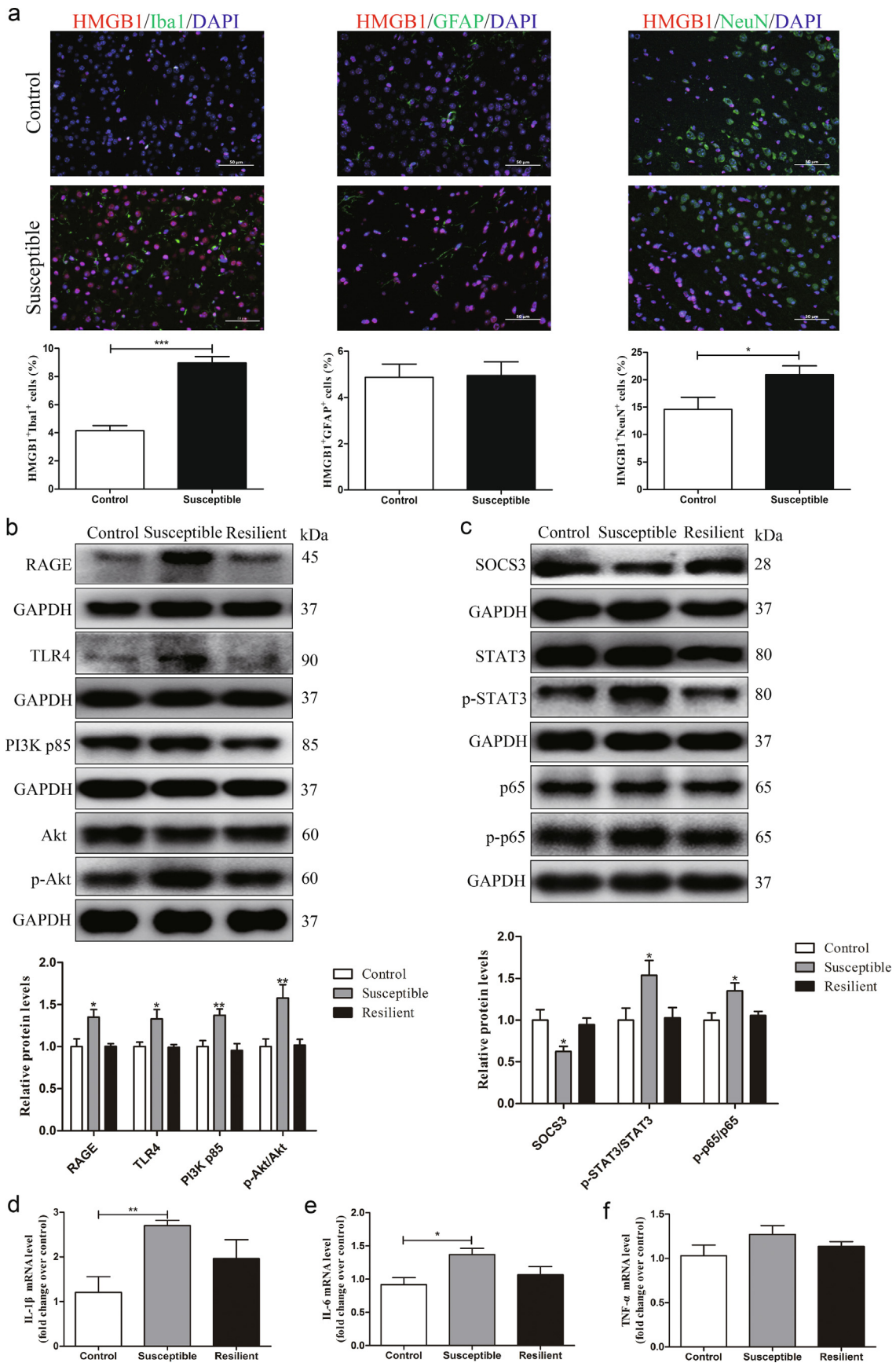


**Fig. 4.** Chronic social defeat stress (CSDS) promotes microglial HMGB1/STAT3/p65 axis expression in the mPFC of susceptible mice. (a) Representative immunofluorescence images showing and densitometric analysis of the percentage of HMGB1 in Iba1-positive cells (green; microglia), GFAP-positive cells (green; astrocytes), and NeuN-positive cells (green; neurons) in the mPFC of control and CSDS-susceptible mice ( $n = 3$  per group; scale bar, 50  $\mu\text{m}$ ). Cell nuclei are counterstained blue with 4,6-diamidino-2-phenylindole (DAPI). (b, c) Expression levels of HMGB1 downstream proteins in the mPFC ( $n = 4$  per group), including RAGE, TLR4, PI3K p85, p-Akt/Akt, SOCS3, p-STAT3/STAT3, and p-p65/p65. (d–f) mRNA levels of IL-1 $\beta$  (d), IL-6 (e), and TNF- $\alpha$  (f) in the mPFC ( $n = 5$  per group). Data are presented as mean  $\pm$  SEM. \* $P < 0.05$ , \*\* $P < 0.01$ , \*\*\* $P < 0.001$  vs. control group.

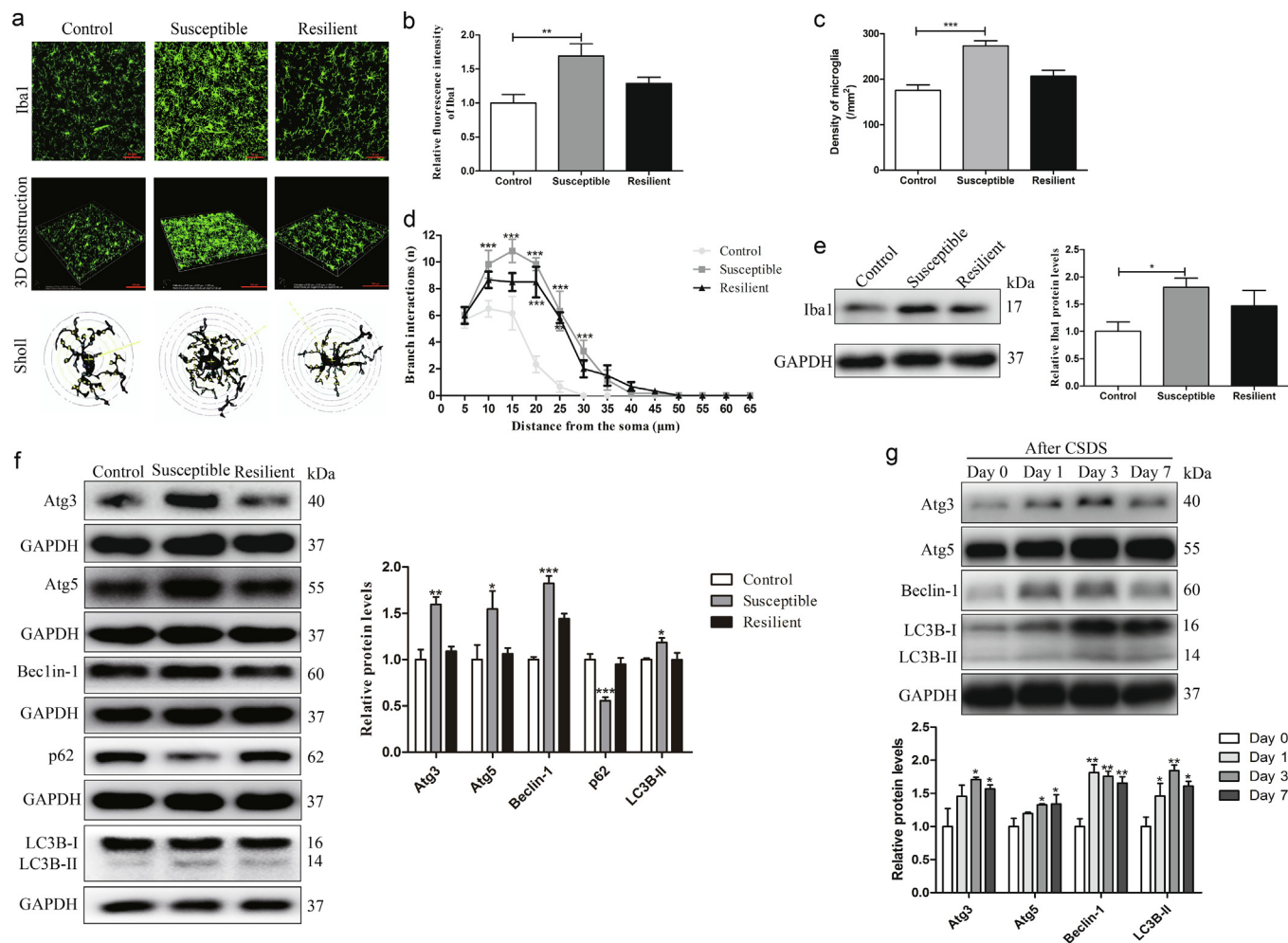


**Fig. 5.** Chronic social defeat stress (CSDS) treatment results in increased microglial activation and autophagy in the mPFC of susceptible mice. (a) Representative immunofluorescence images of Iba1 within the mPFC (scale bar, 50  $\mu$ m), three-dimensional (3D) construction (scale bar, 100  $\mu$ m), and Sholl analysis in each group. (b–d) Iba1 fluorescence intensity (b), the density of microglia (c), and Sholl analysis for branch interactions as a function of distance from the soma (d) in the mPFC ( $n = 3$  per group). (e) Iba1 expression level in the mPFC ( $n = 3$  per group). (f) Expression levels of autophagy markers Atg3, Atg5, Beclin-1, p62, and LC3B-II in the mPFC ( $n = 4$  per group). (g) Expression levels of Atg3, Atg5, Beclin-1, and LC3B-II in the mPFC of susceptible mice at day 0, day 1, day 3, and day 7 after CSDS ( $n = 4$  per group). Data are presented as mean  $\pm$  SEM. \* $P < 0.05$ , \*\* $P < 0.01$ , \*\*\* $P < 0.001$  vs. indicated group.

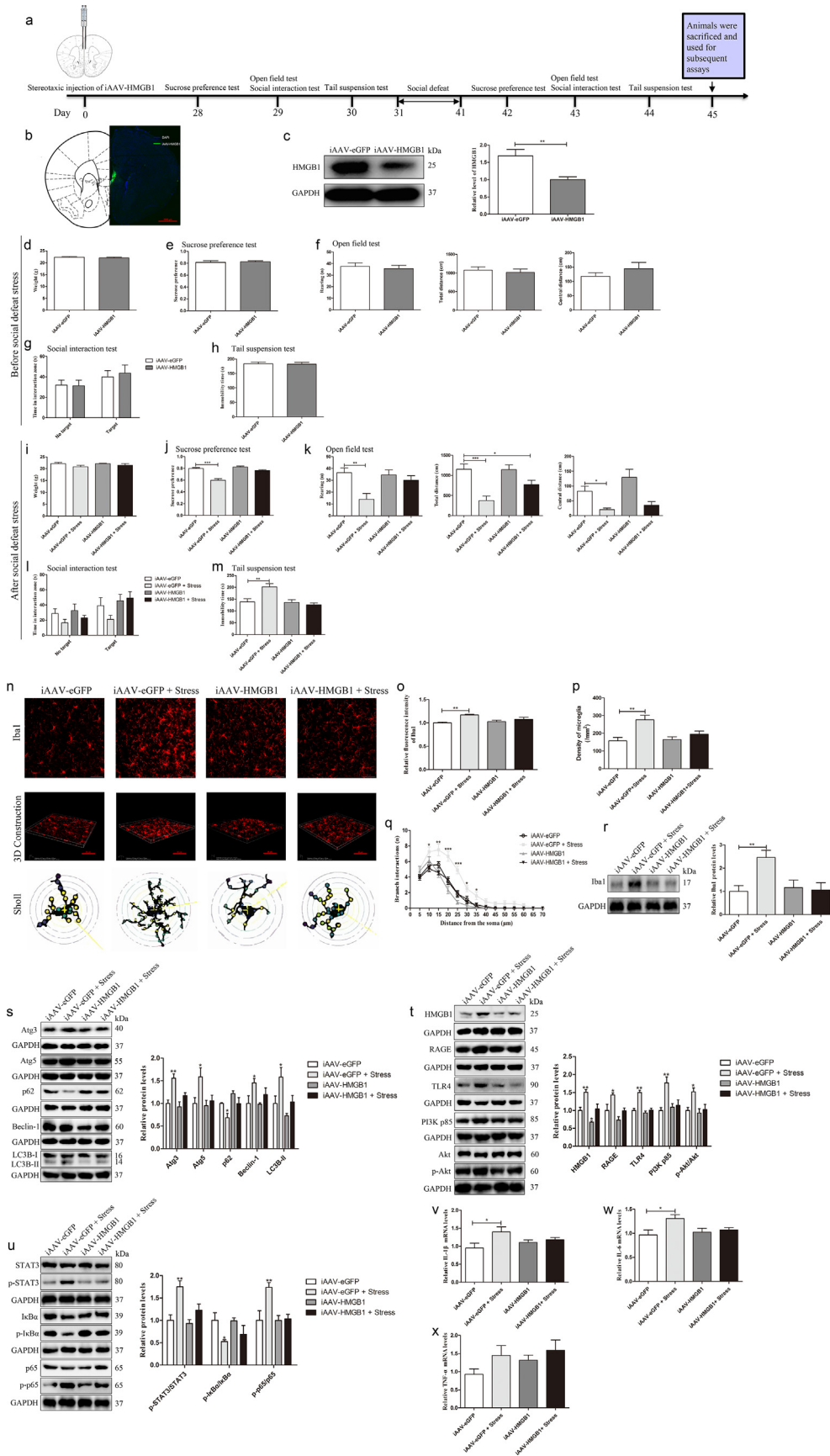
LC3B-II were significantly increased, whereas SQSTM1/p62 expression level was reduced in susceptible mice (all  $P < 0.05$ ; Fig. 5f). None of these changes were observed in resilient mice. Furthermore, as autophagy activation in response to acute stress is part of normal physiological responses, and may not necessarily reflect the pathophysiology caused by CSDS, we also examined the autophagy activity in susceptible mice after CSDS with an additional timeline. We found that the expression of Atg3, Atg5, Beclin-1, and LC3B-II were increased, mostly peaking between 1 and 3 days and remaining elevated at day 7 post-CSDS in susceptible mice (all  $P < 0.05$  vs. Day 0 group; Fig. 5g).

These results suggest that the depressive phenotypes of susceptible mice may have resulted from enhanced HMGB1/STAT3/p65 axis expression in microglial cells in the mPFC and ensuing induction of microglial activation and autophagy.

*Blockade of HMGB1 rescues the depressive-related phenotypes, microglial activation, and autophagy in mice caused by CSDS*

To investigate whether the association between increased HMGB1/STAT3/p65 axis and CSDS was causal, we used an adenovirus-associated virus (AAV)-based strategy. For this purpose, we com-

**Fig. 6.** HMGB1 signaling in the mPFC is necessary and sufficient to promote stress susceptibility. (a) Experimental paradigm for assessing behavior following specific HMGB1 knockdown and chronic social defeat stress (CSDS). (b) Illustration of iAAV-HMGB1 micro-infusion into the mPFC region (scale bar, 1000  $\mu$ m). (c) Knockdown efficiency of HMGB1 shRNA vectors ( $n = 6$  per group). (d–h) Body weight (d), sucrose preference (e), number of rearings, total distance traveled, and central distance traveled in the open field (f), time in the social interaction zone (g), and immobility time during tail suspension (h) in control and iAAV-HMGB1 groups before CSDS ( $n = 22$  per group). (i–m) Corresponding measures after CSDS for iAAV-eGFP ( $n = 11$ ), iAAV-eGFP + Stress ( $n = 9$ ), iAAV-HMGB1 ( $n = 11$ ), and iAAV-HMGB1 + Stress ( $n = 10$ ) groups: body weight (i), sucrose preference (j), open field activity (k), social interaction (l), and immobility time during tail suspension (m). (n) Representative immunofluorescence images of the microglia marker Iba1 within the mPFC (scale bar, 50  $\mu$ m) as well as three-dimensional (3D) construction (scale bar, 50  $\mu$ m) and Sholl analysis of microglia in each group. (o–q) Iba1 fluorescence intensity (o), the density of microglia (p), and Sholl analysis for branch interactions as a function of distance from the soma (q) in each group ( $n = 3$  per group). (r) Iba1 expression level in the mPFC ( $n = 3$  per group). (s) Expression levels of Atg3, Atg5, p62, Beclin-1, and LC3B-II in the mPFC of each group ( $n = 3$  per group). (t) Expression levels of HMGB1, RAGE, TLR4, PI3K p85, and p-Akt/Akt in the mPFC of each group ( $n = 3$  per group). (u) Expression levels of p-STAT3/STAT3, p-IkB $\alpha$ /IkB $\alpha$ , and p-p65/p65 in the mPFC of each group ( $n = 3$  per group). (v–x) RT-qPCR analysis of IL-1 $\beta$  (v), IL-6 (w), and TNF- $\alpha$  (x) expression in the mPFC of each group ( $n = 4$  per group). Data are presented as mean  $\pm$  SEM. \* $P < 0.05$ , \*\* $P < 0.01$ , \*\*\* $P < 0.001$  vs. control group.



pared mice bilaterally injected with iAAV-HMGB1 or a control vector (iAAV-eGFP) (Fig. 6a). As expected, iAAV-HMGB1 infusion into the mPFC (Fig. 6b) significantly reduced HMGB1 expression ( $P < 0.01$ ; Fig. 6c), but did not influence behavioral test performance in mice not exposed to CSDS (all  $P > 0.05$  vs. iAAV-eGFP-injected controls; Fig. 6d–h). However, iAAV-HMGB1 injection prevented depressive-like behaviors following CSDS compared to CSDS-exposed iAAV-eGFP-injected mice, including decreased sucrose consumption in the SPT, number of rearings in the OFT, and central distance traveled in the OFT as well as increased immobility duration in the TST (Fig. 6i–m). Only CSDS-induced reduction of total distance traveled in the OFT was not affected by iAAV-HMGB1 infusion ( $P < 0.05$  vs. iAAV-eGFP-injected controls; Fig. 6k). When compared with the iAAV-eGFP + Stress group, the iAAV-HMGB1 + Stress group had significantly higher sucrose consumption in the SPT, the number of rearings and total distance traveled in the OFT, time in the interaction zone with target in the SIT, and immobility duration in the TST (all  $P < 0.05$ ), though there was no significant difference in the body weight, central distance traveled in the OFT, and time in the interaction zone with target in the SIT (all  $P > 0.05$ ). These findings confirmed that HMGB1 knockdown in mPFC induced stress resilience.

The increases in Iba1 fluorescence intensity, cell density, branch interactions, and expression of Iba1 after CSDS were also mitigated by iAAV-HMGB1 (Fig. 6n–r). And compared with the iAAV-eGFP + Stress group, the iAAV-HMGB1 + Stress group had significantly lower Iba1 fluorescence intensity, cell density, branch interactions, and expression of Iba1 (all  $P < 0.05$ ). Furthermore, iAAV-HMGB1 reversed the CSDS-induced changes in expression levels of the autophagic markers Atg3, Atg5, p62, Beclin-1, and LC3B-II (all  $P > 0.05$  vs. iAAV-eGFP-injected controls but  $P < 0.05$  vs. iAAV-eGFP + Stress group, except for Beclin-1 both  $P > 0.05$  vs. iAAV-eGFP-injected controls and iAAV-eGFP + Stress group; Fig. 6s). iAAV-HMGB1 reversed the effects of CSDS on the expression levels of HMGB1/STAT3/p65 axis in the mPFC (all  $P > 0.05$  vs. iAAV-eGFP-injected controls, but  $P < 0.05$  vs. iAAV-eGFP + Stress group; Fig. 6t, u). Moreover, iAAV-HMGB1 reversed the CSDS-induced changes in mRNA levels of IL-1 $\beta$  and IL-6 (all  $P > 0.05$  vs. iAAV-eGFP-injected controls, but  $P < 0.05$  vs. iAAV-eGFP + Stress group; Fig. 6v, w), while there was no significant change in mRNA level of TNF- $\alpha$  in the iAAV-HMGB1 + Stress group compared to iAAV-eGFP-injected controls or iAAV-eGFP + Stress group (both  $P > 0.05$ ; 6x).

Given the critical role of HMGB1 in the mPFC, we also examined the effects of specific HMGB1 knockdown on local cell proliferation, activity, and survival. HE staining showed that iAAV-HMGB1 did not cause histological changes (Supplementary Fig. S3a). Moreover, HMGB1 knockdown did not significantly alter expression levels of the proliferation markers proliferating cell nuclear antigen and Ki67 as measured by immunohistochemistry (Supplementary Fig. S3b, c), nuclear incorporation of the proliferation marker BrdU as measured by immunofluorescence (Supplementary Fig. S3d), or apoptotic cell numbers as detected by TUNEL staining (Supplementary Fig. S3e).

### STAT3 inhibition abrogated depressive-like behaviors induced by rHMGB1 injection as well as the associated microglial activation and autophagy in mice

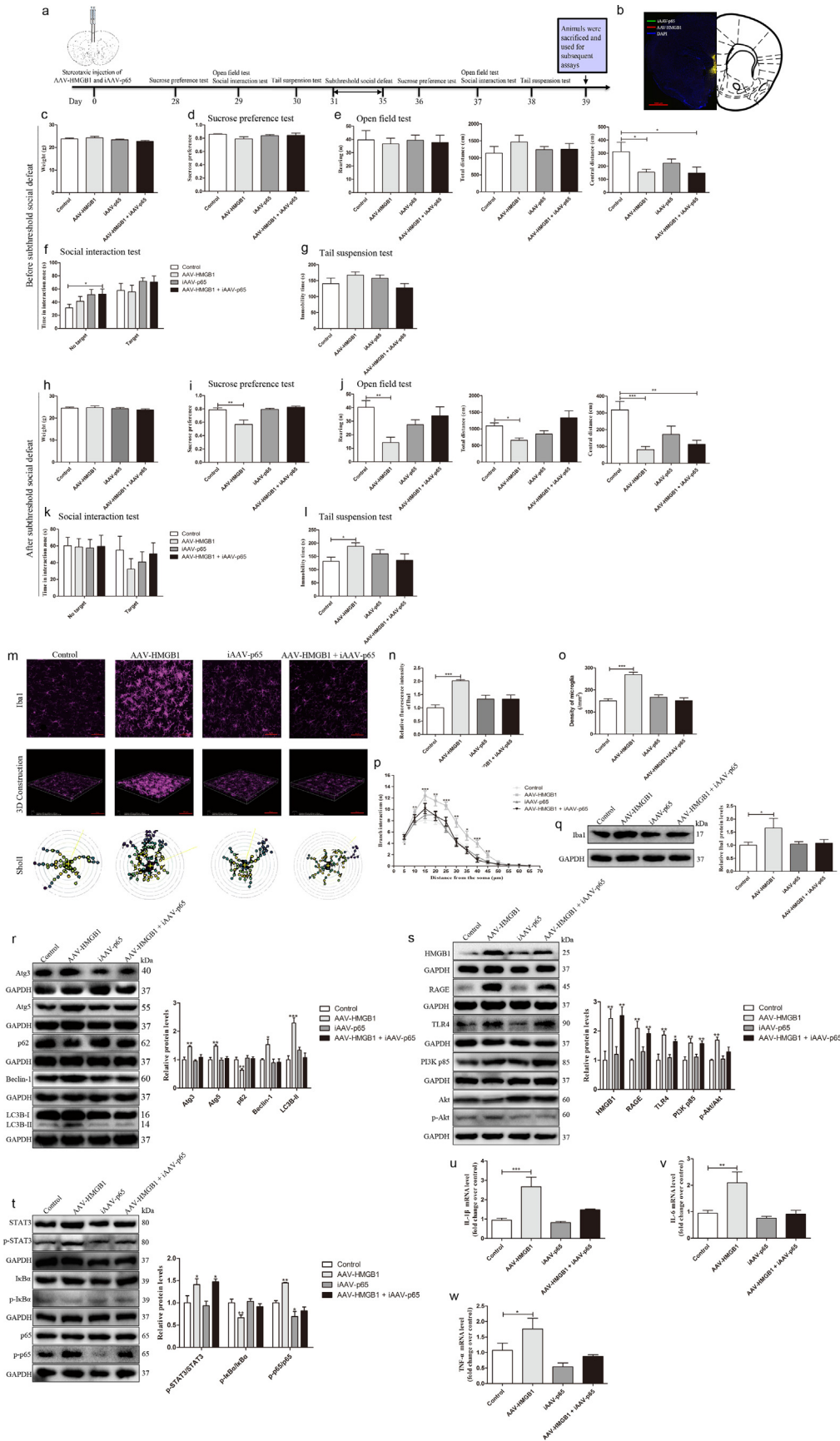
To examine the contributions of HMGB1/STAT3/p65 axis signaling to depressive-like phenotypes, we measured the effects of axis activation by rHMGB1 injection and axis inhibition by Stattic injection on mouse behavior. Based on the previous studies [21,22], 15 mg/kg Stattic (STAT3 specific inhibitor; Selleck Chemicals, Houston, US) was injected intraperitoneally for 1 h before stereotaxic injection of rHMGB1 or PBS (control). At 12 h post-injection, mice were subjected to the SPT, OFT, and TST (Supplementary Fig. S4a). Consistent with induction of an MDD-like phenotype, rHMGB1 injection significantly reduced sucrose consumption in the SPT ( $P < 0.01$ ; Supplementary Fig. S4c) and exploratory activity in the OFT (number of rearings and total distance traveled; all  $P < 0.05$ ; Supplementary Fig. S4d), while increasing immobility duration in the TST ( $P < 0.01$ ; Supplementary Fig. S4e) compared to PBS-injected controls. These depressive-like behaviors were completely reversed by co-treatment with Stattic (all  $P > 0.05$  vs. Control; Supplementary Fig. S4b–e). Meanwhile, compared to the rHMGB1 group, the rHMGB1 + Stattic group had significantly higher sucrose preference in the SPT, the number of rearings and total distance traveled in the OFT, and immobility duration in the TST (all  $P < 0.05$ ).

Moreover, rHMGB1 injection induced robust microglial reactivity in the mPFC as evidenced by significantly increased soma size, cell density, and branch interactions, while these changes were completely blocked by Stattic ( $P > 0.05$  vs. Control; Supplementary Fig. S4f–i). And compared to the rHMGB1 group, the rHMGB1 + Stattic group had significantly lower cell density and branch interactions ( $P < 0.05$ ). In addition, Stattic also mitigated the rHMGB1-induced increases in Atg3, Atg5, and LC3B-II protein expression and the decrease in p62 protein expression within the mPFC (all  $P > 0.05$  vs. Control but  $P < 0.05$  vs. rHMGB1 group; Supplementary Fig. S4j). Though Stattic did not reverse the rHMGB1-induced increases in Beclin-1 ( $P < 0.05$  vs. Control), it was significantly reduced when compared with the rHMGB1 group ( $P < 0.05$ ). Furthermore, Stattic reversed the HMGB1-dependent upregulation of p-STAT3/STAT3, p-p65/p65, IL-1 $\beta$ , and IL-6 (all  $P > 0.05$  vs. Control), but did not affect the rHMGB1-induced increases in HMGB1, RAGE, TLR4, PI3K p85, and p-Akt/Akt (all  $P < 0.05$  vs. Control but  $P > 0.05$  vs. rHMGB1 group) (Supplementary Fig. S4k–o). These findings strongly implicated HMGB1/STAT3/p65 axis signaling in depression-associated microglial activation and autophagy within the mPFC.

### p65 knockdown blocked HMGB1 overexpression-induced depressive-like behaviors, microglial activation, and autophagy in mice

To further investigate the role of HMGB1/STAT3/p65 axis in the development of depression, we also examined the effects of viral HMGB1 overexpression by AAV-HMGB1 injection and p65 knock-

**Fig. 7.** Specific knockdown of p65 in mPFC mitigated depressive-like behavior, microglial activation, and autophagy in HMGB1-overexpressing mice. (a) Experimental timeline. (b) Illustration of AAV-HMGB1 and iAAV-p65 micro-infusions into the mPFC region (scale bar, 1,000  $\mu$ m). (c–g) Mouse body weight (c), sucrose preference (d), number of rearings, total distance traveled, and central distance traveled in the open field (e), time in the social interaction zone (f), and immobility time during tail suspension (g) before subthreshold social defeat stress were measured in control ( $n = 9$ ), AAV-HMGB1 ( $n = 10$ ), iAAV-p65 ( $n = 9$ ), and AAV-HMGB1 + iAAV-p65 ( $n = 10$ ) groups. (h–l) Corresponding results after subthreshold social defeat stress: body weight (h), sucrose preference (i), number of rearings, total distance traveled, and central distance traveled in the open field (j), time in the social interaction zone (k), and immobility time during tail suspension (l) ( $n = 9$  per group). (m) Representative immunofluorescence images of Iba1 within the mPFC (scale bar, 50  $\mu$ m) as well as three-dimensional (3D) reconstruction (scale bar, 50  $\mu$ m) and Sholl analysis of microglia in each group ( $n = 3$  per group). (n, o) Iba1 fluorescence intensity (n) and density of microglia in the mPFC (o). (p) Sholl analysis for branch interactions as a function of distance from the soma. (q) Iba1 expression level in the mPFC ( $n = 3$  per group). (r) Expression levels of Atg3, Atg5, p62, Beclin-1, and LC3B-II in the mPFC ( $n = 3$  per group). (s) Expression levels of HMGB1, RAGE, TLR4, PI3K p85, and p-Akt/Akt in the mPFC ( $n = 3$  per group). (t) Expression levels of p-STAT3/STAT3, p-IkBa/IkBa $\alpha$ , and p-p65/p65 in the mPFC ( $n = 3$  per group). (u–w) mRNA levels of IL-1 $\beta$  (u), IL-6 (v), and TNF- $\alpha$  (w) in the mPFC ( $n = 4$  per group). Data are presented as mean  $\pm$  SEM. \* $P < 0.05$ , \*\* $P < 0.01$ , \*\*\* $P < 0.001$  vs. control group.



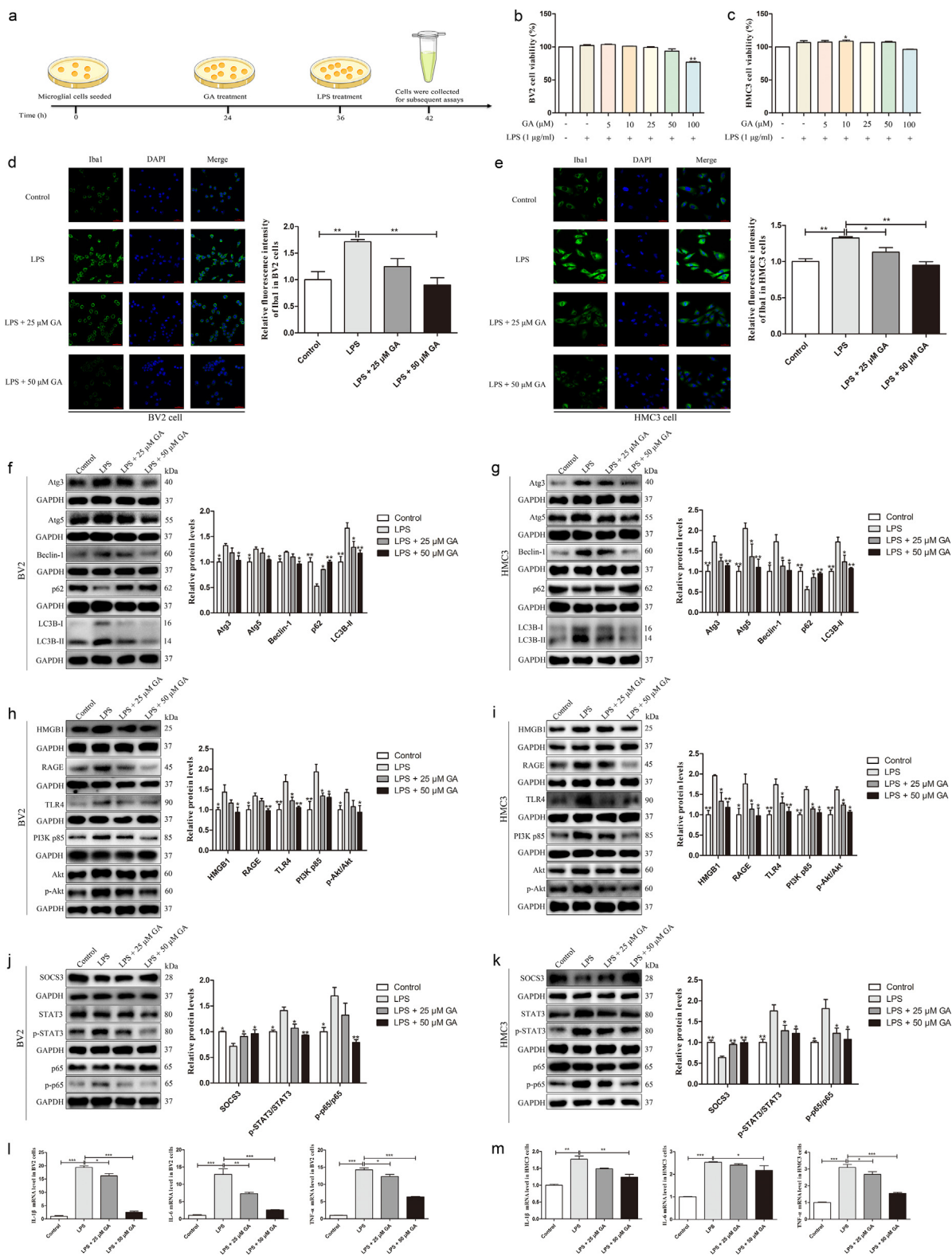


**Fig. 8.** Effects of inhibiting HMGB1 on microglial activation, autophagy, and HMGB1/STAT3/p65 axis expression in cultured microglia after LPS. (a) Experimental timeline of microglia treatment. (b, c) BV2 (b) and HMC3 (c) cells were incubated with different concentrations of glycyrrhizin acid (GA) for 12 h plus LPS to a final concentration of 1 μg/ml for 6 h as indicated, and cell viability was measured using the CCK8 assay ( $n = 3$  per group). (d, e) Example immunofluorescence images and relative fluorescence intensity analysis of Iba1 in BV2 (d) and HMC3 (e) cells treated as indicated ( $n = 3$  per group; scale bar, 50 μm). (f, g) Expression levels of autophagy markers Atg3, Atg5, Beclin-1, p62, and LC3B-II in BV2 (f) and HMC3 (g) cells treated as indicated ( $n = 3$  per group). (h, i) Expression levels of HMGB1, RAGE, TLR4, PI3K p85, and p-Akt/Akt in BV2 (h) and HMC3 (i) cells treated as indicated ( $n = 3$  per group). (j, k) Expression levels of SOCS3, p-STAT3/STAT3, and p-p65/p65 in BV2 (j) and HMC3 (k) cells treated as indicated ( $n = 3$  per group). (l, m) Expression levels of IL-1β, IL-6, and TNF-α mRNAs in BV2 (l) and HMC3 (m) cells treated as indicated ( $n = 4$  per group). Data are presented as mean ± SEM. \* $P < 0.05$ , \*\* $P < 0.01$ , \*\*\* $P < 0.001$  vs. indicated group.

down by iAAV-p65 injection into the mPFC (Fig. 7a). The accuracy of mPFC injection was confirmed by immunofluorescence staining (Fig. 7b). AAV-HMGB1 injection reduced the central distance traveled in the OFT compared to controls ( $P < 0.05$ ), but this effect was not reversed by iAAV-p65 ( $P < 0.05$  vs. Control). Meanwhile, AAV-HMGB1 had no influence on body weight, sucrose preference, number of rearings in the OFT, total distance traveled in the OFT, or immobility time in the TST ( $P > 0.05$  vs. Control; Fig. 7c–g), possibly due to a ceiling effect. However, when compared to the AAV-HMGB1 group, the AAV-HMGB1 + iAAV-p65 group had significantly lower immobility time in the TST ( $P < 0.05$ ), and no significant differences were found in body weight, sucrose preference in the SPT, the number of rearings, total and central distances traveled in the OFT, and times in the interaction zone with no target or target in the SIT between these groups (all  $P > 0.05$ ; Fig. 7c–g). We then used a subthreshold social defeat stress paradigm in these animals, AAV-HMGB1 reduced sucrose consumption in the SPT, the number of rearings in the OFT, and both central and total distances traveled in the OFT, while increasing immobility time in the TST (all  $P < 0.05$ ; Fig. 7h–l). All of these effects except central distance traveled were completely reversed by iAAV-p65 co-treatment (all  $P > 0.05$  vs. Control), while central distance traveled in the OFT was still decreased ( $P < 0.01$  vs. Control). When compared with the AAV-HMGB1 group, the AAV-HMGB1 + iAAV-p65 group had significantly higher sucrose preference in the SPT, the number of rearings and total distance traveled in the OFT, and lower immobility time in the TST (all  $P < 0.05$ ; Fig. 7h–l).

Infection with iAAV-p65 also reversed all signs of AAV-HMGB1-induced microglial activation in the mPFC (all  $P > 0.05$  vs. Control but  $P < 0.05$  vs. AAV-HMGB1; Fig. 7m–q), including the increases in Iba1 fluorescence intensity, cell density, branch interactions, and expression level of Iba1. Moreover, iAAV-p65 reversed AAV-HMGB1-induced a significantly increased protein expression of Atg3, Atg5, Beclin-1, and LC3B-II (all  $P > 0.05$  vs. Control but  $P < 0.05$  vs. AAV-HMGB1; Fig. 7r). Injection of iAAV-p65 also reversed the AAV-HMGB1-induced increases in p-p65/p65, IL-1 $\beta$ , IL-6, and TNF- $\alpha$  expression levels and the reduced expression levels of p62 and p-I $\kappa$ B $\alpha$ /I $\kappa$ B $\alpha$  (all  $P > 0.05$  vs. Control but  $P < 0.05$  vs. AAV-HMGB1 group), but did not affect the AAV-HMGB1-induced increases in HMGB1, RAGE, TLR4, PI3K P85, and p-STAT3/STAT3 (all  $P < 0.05$  vs. Control but  $P > 0.05$  vs. AAV-HMGB1), although the increased expression of p-Akt/Akt was inhibited ( $P > 0.05$  vs. Control but  $P < 0.05$  vs. AAV-HMGB1 group) (Fig. 7s–w). Together, these results further strengthened the notion that HMGB1 in mPFC mediates depression by regulating the HMGB1/STAT3/p65 axis and ensuing microglial activation and autophagy.

#### HMGB1 or NF- $\kappa$ B inhibition eliminates LPS-induced cultured microglial activation and autophagy

To further evaluate the role of HMGB1/STAT3/p65 axis in regulating microglial activation and autophagy, the HMGB1 inhibitor GA, the NF- $\kappa$ B inhibitor pyrrolidinedithiocarbamate ammonium (PDTC), and rHMGB1 were used *in vitro*. At first, we examined the responses of BV2 and HMC3 microglial cell lines to LPS stimulation (1  $\mu$ g/ml for 6 h) in the presence and absence of GA for 12 h (Fig. 8a). Low concentrations of GA (0, 5, 10, 25, 50  $\mu$ M) plus 1  $\mu$ g/ml LPS induced no obvious toxicity in either cell line (Fig. 8b, c). And HMGB1 was predominantly localized in the nucleus of BV2 and HMC3, but translocated and accumulated noticeably in the cytoplasm (Supplementary Fig. S5a, b) with LPS treatment accompanied by the increased release of HMGB1 (Supplementary Fig. S5c, d). In control cultures, LPS increased Iba1 fluorescence intensity, while co-treatment with 50  $\mu$ M GA significantly blocked this response ( $P < 0.01$  vs. treatment; Fig. 8d, e). Moreover, 50  $\mu$ M

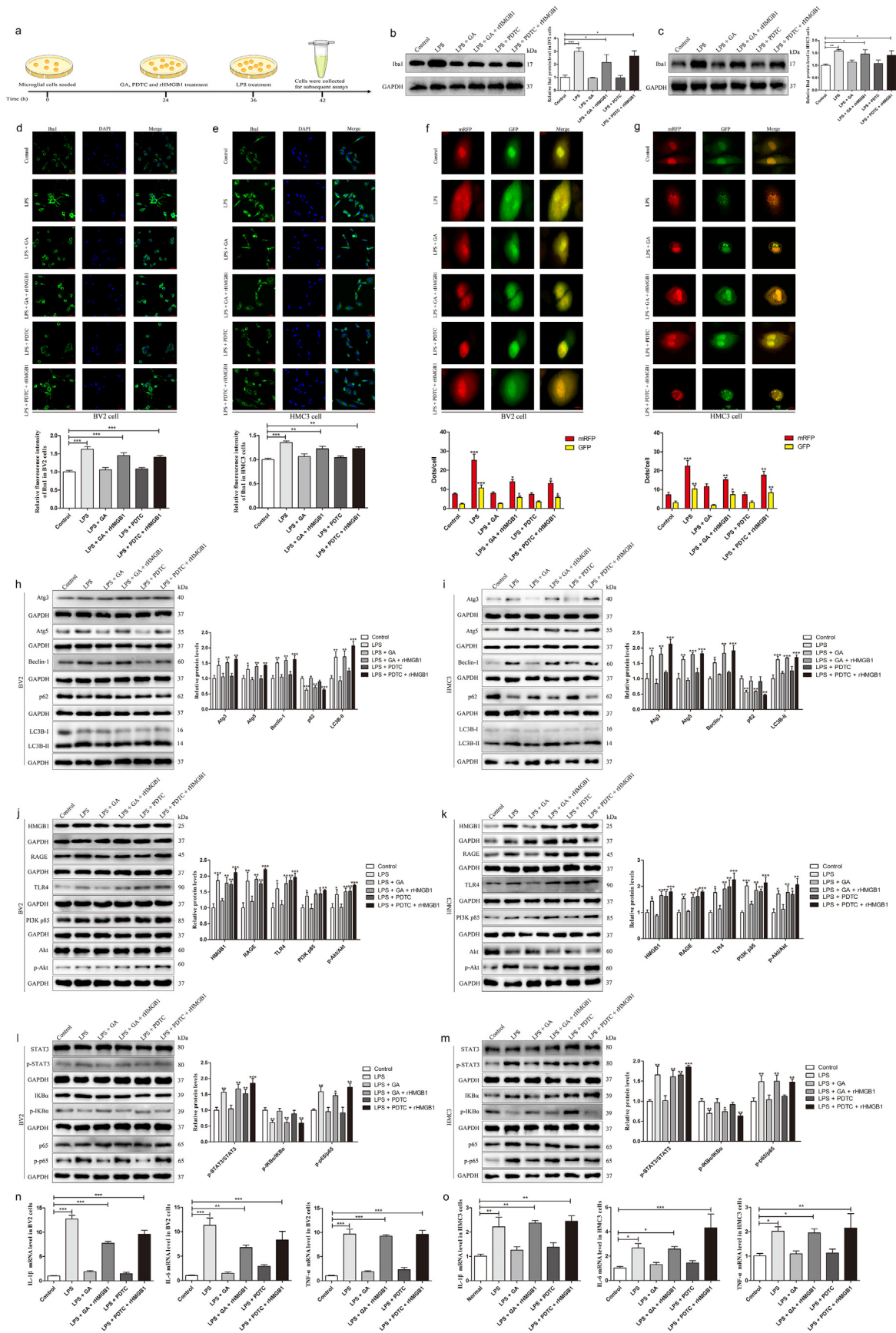
GA reversed the increases in Atg3, Atg5, Beclin-1, and LC3B-II, and the decreases in p62 protein expression induced by LPS (all  $P < 0.05$  vs. LPS treatment; Fig. 8f, g), suggesting that HMGB1 mediated LPS-induced microglial activation and autophagic activity. Western blot analysis revealed that 50  $\mu$ M GA treatment significantly attenuated HMGB1/STAT3/p65 axis activation in LPS-stimulated microglia (all  $P < 0.05$  vs. LPS treatment; Fig. 8h–k). Furthermore, 50  $\mu$ M GA markedly suppressed the LPS-induced increases in IL-1 $\beta$ , IL-6, and TNF- $\alpha$  mRNA expression (all  $P < 0.05$  vs. LPS treatment; Fig. 8l, m). Thus, inhibiting HMGB1 eliminated the LPS-induced increases in HMGB1/STAT3/p65 axis activity and pro-inflammatory cytokines expression in cultured microglia.

We further examined the effects of rHMGB1 (10 ng/ml for 12 h) in the presence and absence of 50  $\mu$ M GA or 5  $\mu$ M of PDTC for 12 h on BV2 and HMC3 cell's response to LPS (1  $\mu$ g/ml for 6 h) (Fig. 9a). Notably, 5  $\mu$ M PDTC plus 1  $\mu$ g/ml LPS induced no obvious toxicity ( $P > 0.05$ ; Supplementary Fig. S6a, b), and RT-qPCR showed that co-administration of 10 ng/ml rHMGB1 reversed the suppressive effects of 50  $\mu$ M GA on LPS-induced activation of HMGB1 ( $P < 0.05$ ; Supplementary Fig. S6c, d). GA and PDTC significantly inhibited the LPS-induced upregulation of the Iba1 protein level (Fig. 9b, c). And immunofluorescence analysis showed that the LPS-induced increase in Iba1 fluorescence intensity ( $P < 0.001$ ) was attenuated by treatment with either GA or PDTC (all  $P > 0.05$  vs. control; Fig. 9d, e). Moreover, microglial autophagic flux analysis indicated that the increases in autolysosome and autophagosome numbers induced by LPS ( $P < 0.01$ ) were attenuated by either HMGB1 or NF- $\kappa$ B inhibition (all  $P > 0.05$  vs. control; Fig. 9f, g). Inhibiting the HMGB1/STAT3/p65 axis significantly reduced LPS-induced upregulation of the autophagic marker proteins Atg3, Atg5, Beclin-1, and LC3B-II, and downregulation of p62 (all  $P > 0.05$  vs. control; Fig. 9h, i). PDTC also significantly attenuated the LPS-induced increases in p-p65/p65 expression as well as the decreases in p-I $\kappa$ B $\alpha$ /I $\kappa$ B $\alpha$  expression (all  $P > 0.05$  vs. control), but did not reverse the LPS-induced increases in HMGB1, RAGE, TLR4, PI3K p85, p-Akt/Akt, and p-STAT3/STAT3 expression (Fig. 9j–m). Furthermore, LPS-induced increases in IL-1 $\beta$ , IL-6, and TNF- $\alpha$  expression were attenuated by inhibiting the HMGB1/STAT3/p65 axis (all  $P > 0.05$  vs. control; Fig. 9n, o). Conversely, rHMGB1 co-treatment mitigated these suppressive effects of GA and PDTC on LPS-induced microglial activation, autophagosome accumulation, and upregulation of the HMGB1/STAT3/p65 axis (Fig. 9b–o). These results suggest that the HMGB1/STAT3/p65 axis was necessary for LPS-induced microglial activation and autophagy.

## Discussion

To the best of our knowledge, this study is the first report that serum HMGB1 was elevated in MDD patients and positively correlated with symptom severity, and provided the first direct evidence that activation of the HMGB1/STAT3/p65 axis and ensuing microglial activation and autophagy in the mPFC contributed to stress-induced depression.

Analysis of whole-transcriptome expression data identified numerous genes differentially expressed by MDD or MDDs patients compared to healthy controls, as well as four genes differentially expressed by both patient groups. While one of these genes, encoding IL-1A, has been implicated in depressive disorder [23], the other three are novel and merit investigation in the future. Importantly, IPA analysis predicted that MDD was associated with HMGB1/STAT3/p65 axis-induced microglial activation and autophagy in the mPFC. HMGB1 has been recognized as a potent inducer of pro-inflammatory cytokines that contribute to the pathogenesis of diverse neuroinflammatory disorders [24].



Stress-induced inflammation mediated by HMGB1 may also cause motivational deficits, a common feature of psychiatric illnesses such as MDD [25]. Further, chronic neuroinflammation is linked to increased microglial activation, and HMGB1 can be actively secreted from reactive microglia in the brain [26]. Neuroinflammation also would interact with and influence autophagy via immunophenotypic switching of microglia [27].

Interestingly, in the present study, considering the obvious effect of estrogen on the development of MDD [28], we only studied the whole-transcriptome expression data from male samples. Previous studies have reported that HMGB1 is regulated by the steroid hormone estrogen [29,30], which indirectly supports the reliability of our results and the reasonability that we excluded the female data. However, females had a higher incidence of MDD than males [31], analysis of the whole-transcriptome expression data including males and females should be conducted and compared with present results in the future.

Here, we showed that serum HMGB1 levels could distinguish HCs from MDD, and high levels of HMGB1 in serum positively correlated with MDD severity, which indicates that HMGB1 may be a potential biomarker for severe MDD due to its relative stability in blood and ability to be rapidly and inexpensively measured. Moreover, changes in total brain HMGB1 during neurological conditions may be mirrored in the blood as many such conditions involve disruption of the blood–brain barrier (BBB) [32]. The anti-HMGB1 monoclonal antibody could inhibit HMGB1 release into the brain extracellular space and reduce serum HMGB1 by protecting BBB integrity [33]. It has been reported that neurovascular pathology mediates stress-induced depression [34], and the activated microglia contribute to BBB impairment [35]. We also found that CSDS promoted HMGB1 expression level upregulation and microglial activation in the mPFC, which positively correlated with depressive-like behaviors in mice. And the increased HMGB1 was mainly observed in microglia, further suggesting a critical role of mPFC-derived microglial HMGB1 in CSDS-induced depression. Whether microglial HMGB1-dependent disruption of BBB integrity in the mPFC participates in chronic stress-induced MDD, is a possibility warranting further investigation.

Furthermore, we verified increased autophagy in the mPFC of CSDS model mice, in line with a previous clinical study reported that patients with MDD had elevated levels of the autophagy proteins LC3, ATG12, and Beclin-1 in their peripheral blood mononuclear cells [36]. However, previous studies have also reported both increased [37] and decreased [38] autophagy marker expression in depression-relevant animal models. As well, antidepressants have been reported to both increase autophagy [39] and impair autophagy [40]. These discrepancies may be explained by the methods used to evaluate autophagic induction. The majority of these studies evaluated autophagy by measuring changes in LC3B-II/LC3B-I, which while a widely used autophagic marker, also increases when autophagy is inhibited by blocking the fusion between autophagosomes and lysosomes. The latest guidelines for monitoring autophagy recommend measuring autophagic protein turnover and comparing the levels of LC3B-II to other “housekeeping” proteins rather than LC3B-I [41]. In this study, we also

assessed autophagy activity in the mPFC of stress-susceptible mice after CSDS with an additional timeline, the expression of mostly autophagy markers peaked on day 1 and day 3, further suggesting that CSDS would promote autophagy in the mPFC. However, we observed a decrease in the level of these autophagy markers but remained substantially higher on day 7, which may be due to the excess activation of autophagy-inducing cell death [42]. Considering that the duration of a stress paradigm used in each animal study was different, which may also explain the reported discrepancy. More careful assessment of the experiment timeline, particularly in regard to the duration of stress exposure to animals, may be critical. It is a limitation that we only observed the effects of CSDS (10 days) on autophagy. And CSDS model mice might not fully recapitulate the pathophysiology of human depression. In the future, we need to further investigate the effects of acute and chronic stress on autophagy via different depressive mice models, such as LPS-induced (24 h), CUMS-induced (8 weeks), and so on.

A redox-sensitive cysteine complex, Cys23, Cys45, and Cys106, controls the function of HMGB1. And three isoforms of HMGB1 have been identified, fully reduced HMGB1, disulfide-HMGB1, and sulphonyl-HMGB1 [43]. The fully reduced form of HMGB1 stimulates autophagy through its interaction with RAGE, while the disulfide-HMGB1 causes pro-inflammatory effects by binding to TLR4. Moreover, under oxidative stress, the Cys23-Cys45 intramolecular disulfide bond induces HMGB1 nucleocytoplasmic translocation and secretion, a process that also requires Cys106 [12]. Extracellular disulfide-HMGB1 would activate several signal-transduction pathways, including PI3K and NF- $\kappa$ B pathways, and consequently induce pro-inflammatory cytokines, such as TNF- $\alpha$ , IL-1 $\beta$ , and IL-6. In addition, autophagy can be regulated by either the NF- $\kappa$ B signaling pathway or its downstream cytokine IL-6 [44]. Moreover, STAT3 is an important regulator of neuroinflammation [45] and autophagy [46]. Thus, there are multiple potential molecular pathways linking HMGB1 signaling, neuroinflammation, and autophagy. A previous study showed that the activation of HMGB1/TLR4/NF- $\kappa$ B signaling pathway in the PFC of CUMS-induced model of depression [47], while we found that the HMGB1 downstream receptors TLR4 and RAGE both were activated in the mPFC of CSDS model mice, suggesting that TLR4 may not be the only key molecule in regulating depression. Meanwhile, in this study, we found that CSDS strongly provoked the activation of STAT3, which was similar to a previous study [48]. And it has been reported that microglial-specific STAT3 knockout mice showed anti-depressive-like behavior [49]. These results strongly indicated STAT3, especially in microglial, is involved in the induction of depression. Moreover, using *in vivo* and *in vitro* models, our current study revealed an important role for the HMGB1/STAT3/p65 axis in microglial activation and autophagy as well as this response-induced depression.

Specific knockdown of HMGB1 in the mPFC promoted resilience to stress as evidenced by reductions in depressive behaviors as well as downregulation of microglial activity and autophagy markers. Meanwhile, HMGB1 knockdown would not affect local cell viability in the mPFC, consistent with a previous report that the lack of chromosomal HMGB1 protein did not disrupt cell growth [50].

**Fig. 9.** Inhibition of HMGB1/STAT3/p65 axis eliminates LPS-induced microglial activation and autophagy in culture. (a) Experimental timeline of microglial treatment. (b, c) Expression levels of Iba1 in BV2 cells (b) and HMC3 cells (c) treated as indicated ( $n = 4$  per group). (d, e) Example immunofluorescence images (scale bar, 50  $\mu$ m) and relative fluorescence intensity analysis of Iba1 in BV2 cells (d) and HMC3 cells (e) treated as indicated ( $n = 3$  per group). (f, g) Example immunofluorescence images (scale bar, 20  $\mu$ m) and quantitative results for mRFP-GFP-LC3 stably transfected BV2 cells (f) and HMC3 cells (g) treated as indicated. (h, i) Expression levels of autophagy markers Atg3, Atg5, Beclin-1, p62, and LC3B-II in BV2 cells (h) and HMC3 cells (i) treated as indicated ( $n = 4$  per group). (j, k) Expression levels of HMGB1, RAGE, TLR4, PI3K p85, and p-Akt/Akt in BV2 cells (j) and HMC3 cells (k) treated as indicated ( $n = 4$  per group). (l, m) Expression levels of p-STAT3/STAT3, p-I $\kappa$ B $\alpha$ /I $\kappa$ B $\alpha$ , and p-p65/p65 in BV2 cells (l) and HMC3 cells (m) treated as indicated ( $n = 4$  per group). (n, o) Expression levels of IL-1 $\beta$ , IL-6, and TNF- $\alpha$  mRNAs in BV2 cells (n) and HMC3 cells (o) treated as indicated ( $n = 4$  per group). Data are presented as mean  $\pm$  SEM. \* $P < 0.05$ , \*\* $P < 0.01$ , \*\*\* $P < 0.001$  vs. control group.

These results also further validate that HMGB1 knockout mice are viable only for a short time after birth independent of cell viability. Furthermore, micro-infusion of rHMGB1 or AAV-HMGB1 overexpression into the mPFC induced depressive-like behaviors, microglial activation, and autophagy. These effects were blocked by pharmacological inhibition of STAT3 or genetic inhibition of p65, suggesting that the HMGB1/STAT3/p65 axis signaling was not only necessary but also sufficient for some depressive phenotypes. However, HMGB1 knockdown did not completely reverse stress-induced anxiety-like behaviors, and p65 knockdown also would not effectively reverse HMGB1 overexpression-induced anxiety-like behaviors. These results suggested mechanistically distinct pathways regulating anxiety and depression induced by HMGB1. Although depression and anxiety are highly comorbid in the clinic, they demonstrate distinct risk factor profiles, clinical courses, and treatment responses. Thus, the microglial HMGB1/STAT3/p65 axis does not appear to be essential for chronic stress-induced anxiety disorder.

*In vitro*, we identified that HMGB1 was translocated and accumulated noticeably in the microglial cytoplasm after LPS treatment, accompanied by increased release of HMGB1. The findings here were similar to some previous studies [21,51], indicating that stress contributes to the development of MDD, which might predominantly be by facilitating nucleocytoplasmic translocation and active release of HMGB1. Moreover, inhibition of the STAT3/NF- $\kappa$ B axis significantly reduced microglial activation [52], and NF- $\kappa$ B activation correlated with IL-6-mediated autophagy [44]. GA acts as a neuroprotectant by inhibiting HMGB1 expression as well as by downregulating the expression of pro-inflammatory cytokines [53]. Our current *in vitro* study found that both GA and PDTC separately reduced LPS-induced microglial hyper-ramification, autophagy, and pro-inflammatory cytokines overexpression, while rHMGB1 significantly reversed these effects. These results strongly supported HMGB1 as a major activator of the STAT3/NF- $\kappa$ B signaling pathway and ensuing microglial reactivity and autophagy. However, there are several different cell types in the mPFC, all of which exert distinct functions during microglial activation and autophagy under stress. Bidirectional neuron-glia interactions also contribute to the neurobiological process underlying depression [54]. Thus, it was also a limitation that we only assessed cultured microglia *in vitro*. Additional studies using mixed cultures are needed to further assess potential intermediary influences of other cells, such as neurons and astrocytes. In addition, considering that we have verified that rHMGB1 promoted microglial activation and autophagy *in vivo*, and LPS would induce the HMGB1 released, here we did not examine the direct effects of rHMGB1 in microglial *in vitro*. Though it is not necessary and would not affect the conclusion, further study is also needed in the future.

## Conclusions

This study aimed to elucidate the underlying mechanisms by which dysregulated neuroinflammation and autophagy induce MDD. Depending on the re-analyzed whole-transcriptome expression results for the dlPFC of post-mortem male MDD patients, the HMGB1/STAT3/p65 axis was identified as a potential pathway mediating MDD-associated microglial activation and autophagy. HMGB1 level was elevated in the serum of MDD patients and in the mPFC of chronic social defeat stress-induced depression model mice, and positively correlated with symptom severity. HMGB1 may also act as a biomarker for MDD. Moreover, an increased HMGB1/STAT3/p65 axis expression, microglial activation, and autophagy were observed in the mPFC of MDD model mice, and the increased expression of HMGB1 was mainly observed in micro-

glia. Additionally, *in vivo* and *in vitro* analysis fully validate the critical role of HMGB1/STAT3/p65 axis-mediated microglial activation and autophagy in chronic stress-induced MDD. Our work shows that the microglial HMGB1/STAT3/p65 axis in mPFC directly mediates microglial activation and autophagy in depression, highlighting the blocking of microglial HMGB1 signaling within the mPFC may represent a novel therapeutic strategy for treating MDD in chronically stressed individuals.

## Compliance with Ethics Requirements

This study was approved by the Ethics Committee of Chongqing Medical University (No.2017013). Experiments involving humans were performed in accordance with the Code of Ethics of the World Medical Association (Declaration of Helsinki) and informed consent was obtained from the patients and healthy donors before blood sampling in the study. All animal experiments were carried out according to the U.K. Animals (Scientific Procedures) Act, 1986 compliance with the ARRIVE guidelines.

## CRediT authorship contribution statement

**Ke Xu:** Conceptualization, Investigation, Methodology, Data curation, Formal analysis, Writing – original draft. **Mingyang Wang:** Methodology, Investigation, Data curation. **Haiyang Wang:** Methodology, Investigation, Validation. **Shuang Zhao:** Methodology, Investigation, Validation. **Dianji Tu:** Investigation, Validation. **Xue Gong:** Methodology, Investigation. **Wenxia Li:** Investigation, Validation. **Xiaolei Liu:** Visualization. **Lianmei Zhong:** Supervision, Conceptualization, Writing – review & editing, Visualization. **Jianjun Chen:** Supervision, Conceptualization, Writing – review & editing, Formal analysis. **Peng Xie:** Supervision, Conceptualization, Writing – review & editing, Funding acquisition.

## Declaration of Competing Interest

The authors declare that they have no known competing financial interests or personal relationships that could have appeared to influence the work reported in this paper.

## Appendix A. Supplementary material

Supplementary data to this article can be found online at <https://doi.org/10.1016/j.jare.2023.06.003>.

## References

- [1] Smith K. Mental health: a world of depression. *Nature* 2014;515(7526):181. doi: <https://doi.org/10.1038/515180a>.
- [2] Meier TB, Drevets WC, Wurfel BE, Ford BN, Morris HM, Victor TA, et al. Relationship between neurotoxic kynurenine metabolites and reductions in right medial prefrontal cortical thickness in major depressive disorder. *Brain Behav Immun* 2016;53:39–48. doi: <https://doi.org/10.1016/j.bbi.2015.11.003>.
- [3] Belleau EL, Treadway MT, Pizzagalli DA. The Impact of Stress and Major Depressive Disorder on Hippocampal and Medial Prefrontal Cortex Morphology. *Biol Psychiatry* 2019;85(6):443–53. doi: <https://doi.org/10.1016/j.biopsych.2018.09.031>.
- [4] Seamans JK, Lapish CC, Durstewitz D. Comparing the prefrontal cortex of rats and primates: insights from electrophysiology. *Neurotox Res* 2008;14(2–3):249–62. doi: <https://doi.org/10.1007/BF03033814>.
- [5] Mok SW-F, Wong VK-W, Lo H-H, de Seabra Rodrigues Dias IR, Leung EL-H, Law BY-K, et al. Natural products-based polypharmacological modulation of the peripheral immune system for the treatment of neuropsychiatric disorders. *Pharmacol Therap* 2020;208:107480. doi: <https://doi.org/10.1016/j.pharmthera.2020.107480>.
- [6] Puri D, Subramanyam D. Stress – (self) eating: Epigenetic regulation of autophagy in response to psychological stress. *FEBS J* 2019;286(13):2447–60. doi: <https://doi.org/10.1111/febs.14826>.
- [7] Ali T, Rahman SU, Hao Q, Li W, Liu Z, Ali Shah F, et al. Melatonin prevents neuroinflammation and relieves depression by attenuating autophagy impairment through FOXO3a regulation. *J Pineal Res* 2020;69(2):e12667.

- [8] Jiang G, Wang Y, Liu Q, Gu T, Liu S, Yin A, et al. Autophagy: A New Mechanism for Esketamine as a Depression Therapeutic. *Neuroscience* 2022;498:214–23. doi: <https://doi.org/10.1016/j.neuroscience.2022.05.014>.
- [9] Cui WY, Ning YP, Hong W, Wang J, Liu ZN, Li MD. Crosstalk Between Inflammation and Glutamate System in Depression: Signaling Pathway and Molecular Biomarkers for Ketamine's Antidepressant Effect. *Mol Neurobiol* 2019;56(5):3484–500. doi: <https://doi.org/10.1007/s12035-018-1306-3>.
- [10] Setiawan E, Attwells S, Wilson A, Mizrahi R, Rusjan P, Miler L, et al. Association of translocator protein total distribution volume with duration of untreated major depressive disorder: a cross-sectional study. *Lancet Psychiatry* 2018;5(4):339–47. doi: [https://doi.org/10.1016/s2215-0366\(18\)30048-8](https://doi.org/10.1016/s2215-0366(18)30048-8).
- [11] Li J, Kokkola R, Tabibzadeh S, Yang R, Ochani M, Qiang X, et al. Structural basis for the proinflammatory cytokine activity of high mobility group box 1. *Mol Med* 2003;9:37–45.
- [12] Kwak MS, Kim HS, Lee B, Kim YH, Son M, Shin J-S. Immunological Significance of HMGB1 Post-Translational Modification and Redox Biology. *Front Immunol* 2020;11:1189. doi: <https://doi.org/10.3389/fimmu.2020.01189>.
- [13] Pérez-Carrión M, Ceña V. Knocking Down HMGB1 Using Dendrimer-Delivered siRNA Unveils Its Key Role in NMDA-Induced Autophagy in Rat Cortical Neurons. *Pharm Res* 2013;30(10):2584–95. doi: <https://doi.org/10.1007/s11095-013-1049-9>.
- [14] Wang B, Lian YJ, Su WJ, Peng W, Dong X, Liu LL, et al. HMGB1 mediates depressive behavior induced by chronic stress through activating the kynurenine pathway. *Brain Behav Immun* 2018;72:51–60. doi: <https://doi.org/10.1016/j.bbi.2017.11.017>.
- [15] Lian YJ, Gong H, Wu TY, Su WJ, Zhang Y, Yang YY, et al. Ds-HMGB1 and fr-HMGB1 induce depressive behavior through neuroinflammation in contrast to nonoxid-HMGB1. *Brain Behav Immun* 2017;59:322–32. doi: <https://doi.org/10.1016/j.bbi.2016.09.017>.
- [16] Ramaker MJ, Dulawa SC. Identifying fast-onset antidepressants using rodent models. *Mol Psychiatry* 2017;22(5):656–65. doi: <https://doi.org/10.1038/mp.2017.36>.
- [17] Corbett BF, Luz S, Arner J, Pearson-Leary J, Sengupta A, Taylor D, et al. Sphingosine-1-phosphate receptor 3 in the medial prefrontal cortex promotes stress resilience by reducing inflammatory processes. *Nat Commun* 2019;10(1):3146. doi: <https://doi.org/10.1038/s41467-019-10904-8>.
- [18] Pantazatos SP, Huang YY, Rosoklija GB, Dwork AJ, Arango V, Mann JJ. Whole-transcriptome brain expression and exon-usage profiling in major depression and suicide: evidence for altered glial, endothelial and ATPase activity. *Mol Psychiatry* 2017;22(5):760–73. doi: <https://doi.org/10.1038/mp.2016.130>.
- [19] Rasmussen AL, Okumura A, Ferris MT, Green R, Feldmann F, Kelly SM, et al. Host genetic diversity enables Ebola hemorrhagic fever pathogenesis and resistance. *Science* 2014;346(6212):987–91. doi: <https://doi.org/10.1126/science.1259595>.
- [20] Xu K, Wang MY, Zhou W, Pu JC, Wang HY, Xie P. Chronic d-ribose and d-mannose overload induce depressive/anxiety-like behavior and spatial memory impairment in mice. *Transl Psychiatry* 2021;11(1):90. doi: <https://doi.org/10.1038/s41398-020-01126-4>.
- [21] Elfeky M, Kaede R, Okamoto-Ogura Y, Kimura K. Adiponectin Inhibits LPS-Induced HMGB1 Release through an AMP Kinase and Heme Oxygenase-1-Dependent Pathway in RAW 264 Macrophage Cells. *Mediators Inflamm* 2016;2016:5701959. doi: <https://doi.org/10.1155/2016/5701959>.
- [22] Alhazzani K, Ahmad S, Al-Harbi N, Attia S, Bakheet S, Sarawi W, et al. Pharmacological Inhibition of STAT3 by Stat3 Ameliorates Clinical Symptoms and Reduces Autoinflammation in Myeloid, Lymphoid, and Neuronal Tissue Compartments in Relapsing-Remitting Model of Experimental Autoimmune Encephalomyelitis in SJL/J Mice. *Pharmaceutics* 2021;13(7):925. doi: <https://doi.org/10.3390/pharmaceutics13070925>.
- [23] Lin P, Ding BY, Wu YQ, Dong K, Li QT. Mitogen-stimulated cell proliferation and cytokine production in major depressive disorder patients. *BMC Psychiatry* 2018;18(1):330. doi: <https://doi.org/10.1186/s12888-018-1906-5>.
- [24] Lotze MT, Tracey KJ. High-mobility group box 1 protein (HMGB1): nuclear weapon in the immune arsenal. *Nat Rev Immunol* 2005;5(4):331–42. doi: <https://doi.org/10.1038/nri1594>.
- [25] Zhang H, Ding L, Shen T, Peng D. HMGB1 involved in stress-induced depression and its neuroinflammatory priming role: a systematic review. *General Psychiatry* 2019;32(4):e100084.
- [26] Sun L, Li M, Ma X, Feng HY, Song JL, Lv C, et al. Inhibition of HMGB1 reduces rat spinal cord astrocyte swelling and AQP4 expression after oxygen-glucose deprivation and reoxygenation via TLR4 and NF-κB signaling in an IL-6-dependent manner. *J Neuroinflammation* 2017;14(1):231. doi: <https://doi.org/10.1186/s12974-017-1008-1>.
- [27] Carloni S, Favrais G, Saliba E, Albertini MC, Chalon S, Longini M, et al. Melatonin modulates neonatal brain inflammation through endoplasmic reticulum stress, autophagy, and miR-34a/silent information regulator 1 pathway. *J Pineal Res* 2016;61(3):370–80. doi: <https://doi.org/10.1111/jpi.12354>.
- [28] Newhouse P, Albert K. Estrogen, Stress, and Depression: A Neurocognitive Model. *JAMA Psychiat* 2015;72(7):727–9. doi: <https://doi.org/10.1001/jamapsychiatry.2015.0487>.
- [29] Borrmann L, Kim I, Schultheiss D, Rogalla P, Bullerdiek J. Regulation of the expression of HMGB1, a co-activator of the estrogen receptor. *Anticancer Res* 2001;21(1A):301–5.
- [30] Romine L, Wood J, Lamia L, Prendergast P, Edwards D, Nardulli A. The high mobility group protein 1 enhances binding of the estrogen receptor DNA binding domain to the estrogen response element. *Mol Endocrinol* 1998;12(5):664–74. doi: <https://doi.org/10.1210/mend.12.5.0111>.
- [31] Bhattacharyya S, Ahmed A, Arnold M, Liu D, Luo C, Zhu H, et al. Metabolomic signature of exposure and response to citalopram/escitalopram in depressed outpatients. *Transl Psychiatry* 2019;9(1):173. doi: <https://doi.org/10.1038/s41398-019-0507-5>.
- [32] Festoff BW, Sajja RK, van Dreden P, Cucullo L. HMGB1 and thrombin mediate the blood-brain barrier dysfunction acting as biomarkers of neuroinflammation and progression to neurodegeneration in Alzheimer's disease. *J Neuroinflamm* 2016;13(1):194. doi: <https://doi.org/10.1186/s12974-016-0670-z>.
- [33] Okuma Y, Liu K, Wake H, Zhang J, Maruo T, Date I, et al. Anti-high mobility group box-1 antibody therapy for traumatic brain injury. *Ann Neurol* 2012;72(3):373–84. doi: <https://doi.org/10.1002/ana.23602>.
- [34] Menard C, Pfau ML, Hodes GE, Kana V, Wang VX, Bouchard S, et al. Social stress induces neurovascular pathology promoting depression. *Nat Neurosci* 2017;20(12):1752–60. doi: <https://doi.org/10.1038/s41593-017-0010-3>.
- [35] Ni K, Zhu J, Xu X, Liu Y, Yang S, Huang Y, et al. Hippocampal Activated Microglia May Contribute to Blood-Brain Barrier Impairment and Cognitive Dysfunction in Post-Traumatic Stress Disorder-Like Rats. *J Mol Neurosci* 2022;72(5):975–82. doi: <https://doi.org/10.1007/s12031-022-01981-4>.
- [36] Alcocer-Gómez E, Casas-Barquero N, Núñez-Vasco J, Navarro-Pando JM, Bullón P. Psychological status in depressive patients correlates with metabolic gene expression. *CNS Neurosci Ther* 2017;23(10):843–5. doi: <https://doi.org/10.1111/cns.12755>.
- [37] Shu X, Sun Y, Sun X, Zhou Y, Bian Y, Shu Z, et al. The effect of fluoxetine on astrocyte autophagy flux and injured mitochondrial clearance in a mouse model of depression. *Cell Death Dis* 2019;10(8):577. doi: <https://doi.org/10.1038/s41419-019-1813-9>.
- [38] Zhao Z, Zhang L, Guo X-D, Cao L-L, Xue T-F, Zhao X-J, et al. Rosiglitazone Exerts an Anti-depressive Effect in Unpredictable Chronic Mild-Stress-Induced Depressive Mice by Maintaining Essential Neuron Autophagy and Inhibiting Excessive Astrocytic Apoptosis. *Front Mol Neurosci* 2017;10:293. doi: <https://doi.org/10.3389/fnmol.2017.00293>.
- [39] Gullbins A, Schumacher F, Becker KA, Wilker B, Soddemann M, Boldrin F, et al. Antidepressants act by inducing autophagy controlled by sphingomyelinase. *Mol Psychiatry* 2018;23(12):2324–46. doi: <https://doi.org/10.1038/s41380-018-0090-9>.
- [40] Rossi M, Munarriz ER, Bartesaghi S, Milanese M, Dinsdale D, Guerra-Martin MA, et al. Desmethylclomipramine induces the accumulation of autophagy markers by blocking autophagic flux. *J Cell Sci* 2009;122(18):3330–9. doi: <https://doi.org/10.1242/jcs.048181>.
- [41] Daniel J, Klionsky, Amal Kamal Abdel-Aziz, Sara Abdelfatah, Mahmoud Abdellatif, Asghar Abdoli, Steffen Abel, et al. Guidelines for the use and interpretation of assays for monitoring autophagy (4th edition). *Autophagy* 2021;17(1):1–382. doi: <https://doi.org/10.1080/15548627.2020.1797280>.
- [42] Galluzzi L, Vicencio J, Kepp O, Tasmir E, Mairui M, Kroemer G. To die or not to die: that is the autophagic question. *Curr Mol Med* 2008;8(2):78–91. doi: <https://doi.org/10.2174/156652408783769616>.
- [43] Paudel YN, Angelopoulou E, Piperi C, Othman I, Shaikh MF. HMGB1-Mediated Neuroinflammatory Responses in Brain Injuries: Potential Mechanisms and Therapeutic Opportunities. *Int J Mol Sci* 2020;21(13):4609. doi: <https://doi.org/10.3390/ijms21134609>.
- [44] Zhang H, Chen Z, Miranda RN, Medeiros LJ, McCarty N. TG2 and NF-κB Signaling Coordinates the Survival of Mantle Cell Lymphoma Cells via IL6-Mediated Autophagy. *Cancer Res* 2016;76(21):6410–23. doi: <https://doi.org/10.1158/0008-5472.CAN-16-0595>.
- [45] Hu Y, Zhang X, Zhang J, Xia X, Li H, Qiu C, et al. Activated STAT3 signaling pathway by ligature-induced periodontitis could contribute to neuroinflammation and cognitive impairment in rats. *J Neuroinflammation* 2021;18:80. doi: <https://doi.org/10.1186/s12974-021-02071-9>.
- [46] Xia Y, Ling X, Hu G, Zhu Q, Zhang J, Li Q, et al. Small extracellular vesicles secreted by human iPSC-derived MSC enhance angiogenesis through inhibiting STAT3-dependent autophagy in ischemic stroke. *Stem Cell Res Ther* 2020;11(1):313. doi: <https://doi.org/10.1186/s13287-020-01834-0>.
- [47] Xu X, Piao HN, Aosai F, Zeng XY, Cheng JH, Cui YX, et al. Arctigenin protects against depression by inhibiting microglial activation and neuroinflammation via HMGB1/TLR4/NF-κB and TNF-α/TNFR1/NF-κB pathways. *Br J Pharmacol* 2020;177(22):5224–45. doi: <https://doi.org/10.1111/bph.15261>.
- [48] Guan X, Wang Q, Liu M, Sun A, Li X. Possible Involvement of the IL-6/JAK2/STAT3 Pathway in the Hypothalamus in Depressive-Like Behavior of Rats Exposed to Chronic Mild Stress. *Neuropsychobiology* 2021;80(4):279–87. doi: <https://doi.org/10.1159/000509908>.
- [49] Kwon S, Han J, Choi M, Kwon Y, Kim S, Yi E, et al. Dysfunction of Microglial STAT3 Alleviates Depressive Behavior via Neuron-Microglia Interactions. *Neuropsychopharmacology* : official publication of the American College of Neuropsychopharmacology 2017;42(10):2072–86. doi: <https://doi.org/10.1038/npp.2017.93>.
- [50] Wang H, Yang H, Czura CJ, Sama AE, Tracey KJ. HMGB1 as a Late Mediator of Lethal Systemic Inflammation. *Am J Respir Crit Care Med* 2001;164:1768–73. doi: <https://doi.org/10.1164/rccm.2106117>.
- [51] Quan H, Bae H, Hur Y, Lee K, Lee C, Jang E, et al. Stearoyl lysophosphatidylcholine inhibits LPS-induced extracellular release of HMGB1 through the G2A/calcium/CaMKKβ/AMPK pathway. *Eur J Pharmacol* 2019;852:125–33. doi: <https://doi.org/10.1016/j.ejphar.2019.02.038>.

- [52] Bhat SA, Goel R, Shukla R, Hanif K. Angiotensin Receptor Blockade Modulates NFkappaB and STAT3 Signaling and Inhibits Glial Activation and Neuroinflammation Better than Angiotensin-Converting Enzyme Inhibition. *Mol Neurobiol* 2016;53(10):6950–67. doi: <https://doi.org/10.1007/s12035-015-9584-5>.
- [53] Paudel YN, Angelopoulou E, Semple B, Piperi C, Othman I, Shaikh MF. Potential Neuroprotective Effect of the HMGB1 Inhibitor Glycyrrhizin in Neurological Disorders. *ACS Chem Neurosci* 2020;11(4):485–500. doi: <https://doi.org/10.1021/acscchemneuro.9b00640>.
- [54] Cui Y, Yang Y, Ni Z, Dong Y, Cai G, Foncelle A, et al. Astroglial Kir4.1 in the lateral habenula drives neuronal bursts in depression. *Nature* 2018;554(7692):323–7. doi: <https://doi.org/10.1038/nature25752>.